Global, national, and urban burdens of paediatric asthma incidence attributable to ambient NO_2 pollution: estimates from global datasets

Pattanun Achakulwisut, Michael Brauer, Perry Hystad, Susan C Anenberg

Summary

Background Paediatric asthma incidence is associated with exposure to traffic-related air pollution (TRAP), but the TRAP-attributable burden remains poorly quantified. Nitrogen dioxide (NO_2) is a major component and common proxy of TRAP. In this study, we estimated the annual global number of new paediatric asthma cases attributable to NO_2 exposure at a resolution sufficient to resolve intra-urban exposure gradients.

Methods We obtained 2015 country-specific and age-group-specific asthma incidence rates from the Institute for Health Metrics and Evaluation for 194 countries and 2015 population counts at a spatial resolution of 250×250 m from the Global Human Settlement population grid. We used 2010–12 annual average surface NO_2 concentrations derived from land-use regression at a resolution of 100×100 m, and we derived concentration-response functions from relative risk estimates reported in a multinational meta-analysis. We then estimated the NO_2-attributable burden of asthma incidence in children aged 1–18 years in 194 countries and 125 major cities at a resolution of 250×250 m.

Findings Globally, we estimated that 4·0 million (95% uncertainty interval [UI] 1·8–5·2) new paediatric asthma cases could be attributable to NO_2 pollution annually; 64% of these occur in urban centres. This burden accounts for 13% (6–16) of global incidence. Regionally, the greatest burdens of new asthma cases associated with NO_2 exposure per 100 000 children were estimated for Andean Latin America (340 cases per year, 95% UI 150–440), high-income North America (310, 140–400), and high-income Asia Pacific (300, 140–370). Within cities, the greatest burdens of new asthma cases associated with NO_2 exposure per 100 000 children were estimated for Lima, Peru (690 cases per year, 95% UI 330–870); Shanghai, China (650, 340–770); and Bogota, Colombia (580, 270–730). Among 125 major cities, the percentage of new asthma cases attributable to NO_2 pollution ranged from 5·6% (95% UI 2·4–7·4) in Orlu, Nigeria, to 48% (25–57) in Shanghai, China. This contribution exceeded 20% of new asthma cases in 92 cities. We estimated that about 92% of paediatric asthma incidence attributable to NO_2 exposure occurred in areas with annual average NO_2 concentrations lower than the WHO guideline of 21 parts per billion.

Interpretation Efforts to reduce NO_2 exposure could help prevent a substantial portion of new paediatric asthma cases in both developed and developing countries, and especially in urban areas. Traffic emissions should be a target for exposure-mitigation strategies. The adequacy of the WHO guideline for ambient NO_2 concentrations might need to be revisited.

Funding George Washington University.

Copyright © 2019 The Author(s). Published by Elsevier Ltd. This is an Open Access article under the CC BY NC ND 4.0 license.

Lancet Planet Health 2019

Published Online
April 10, 2019
http://dx.doi.org/10.1016/S2542-5196(19)30046-4

See Online/Comment
http://dx.doi.org/10.1016/S2542-5196(19)30059-2

Milken Institute School of Public Health, George Washington University, Washington, DC, USA (P Achakulwisut PhD, S C Anenberg PhD); **School of Population and Public Health, The University of British Columbia, Vancouver, BC, Canada** (Prof M Brauer ScD); **Institute for Health Metrics and Evaluation, Seattle, WA, USA** (Prof M Brauer); **and College of Public Health and Human Sciences, Oregon State University, Corvallis, OR, USA** (P Hystad PhD)

Correspondence to:
Dr Susan C Anenberg, Milken Institute School of Public Health, George Washington University, Washington, DC 20052, USA
sanenberg@gwu.edu

Introduction

Global paediatric asthma prevalence has increased strikingly since the 1950s, and asthma is now the most commonly reported non-communicable disease among children worldwide.[1] Over the past decade, several epidemiological studies done in North America, Latin America, Europe, and east Asia have reported associations between traffic-related air pollution (TRAP) exposure and new-onset asthma in children, whereas such associations are less clear in adults.[2–6] Corroborating evidence from toxicological and gene-environment studies have suggested that TRAP causes oxidative injury to the airways, leading to inflammation and remodelling that, in a genetically predisposed individual, could result in asthma development.[7,8] Although the putative agent (or agents) within the TRAP mixture has yet to be identified,[9] epidemiological studies have most often relied on nitrogen dioxide (NO_2) as a proxy, because NO_2 measurements are readily available in many countries, and the variability of TRAP mixture appears to be well characterised by NO_2.[10,11] Results from four meta-analyses of TRAP exposure and paediatric asthma incidence all indicated consistent associations with NO_2, but results were mixed for associations with fine particulate matter ($PM_{2.5}$; appendix).[2–5] Reviews[12,13] done by the US Environmental Protection Agency and Health Canada, published in 2016, also concluded that the overall evidence indicates that a causal relationship probably exists

See Online for appendix

Research in context

Evidence before this study

We searched MEDLINE, PubMed, and Google Scholar to identify meta-analyses of epidemiological studies on traffic-related air pollution (TRAP) exposure and paediatric asthma incidence, using a combination of the search terms "traffic-related air pollution", "asthma incidence" or "asthma development", "meta-analysis", and "child*". We limited the search to studies that pooled results from multiple countries, reported a numerical relative risk (RR) accompanied by an estimate of precision, were written in English, and were published up to March 1, 2018. Nitrogen dioxide (NO_2) is a major component and commonly used proxy of the complex TRAP mixture. The most up-to-date and comprehensive multinational meta-analysis reported an RR of 1·26 (95% uncertainty interval 1·10–1·37) per 10 parts per billion (ppb) of TRAP-related NO_2. The Global Burden of Disease studies have not included air pollution as a risk factor for asthma incidence or prevalence, and the only previous study to have estimated the global burden of paediatric asthma incidence attributable to ambient air pollution relied on exposure datasets with resolutions too coarse to resolve the intra-urban NO_2 variability driven primarily by TRAP. A more recent study done at a resolution of 100 × 100 m for a major city in the UK estimated that 18–24% of all annual paediatric asthma incidence might be attributable to ambient NO_2, suggesting that the global burden of asthma associated with NO_2 exposure might be substantial.

Added value of this study

To our knowledge, this study provides the first global estimate of the annual burden of paediatric asthma incidence attributable to ambient NO_2 pollution at a resolution sufficient to resolve intra-urban and near-roadway exposure gradients (250 × 250 m). We provide estimates for 194 countries and 125 major cities.

Implications of all the available evidence

Our findings suggest that a substantial portion of paediatric asthma incidence could be avoided by reducing NO_2 pollution in both developed and developing countries, especially in urban areas. We estimate that about 97% of children lived and about 92% of new asthma cases attributable to NO_2 occurred in areas with annual average NO_2 concentrations lower than the WHO guideline of 21 ppb, suggesting that the adequacy of this guideline might need to be revisited.

between long-term NO_2 exposure and paediatric asthma development. NO_2 is a secondary pollutant formed mainly from fossil fuel combustion; traffic emissions can contribute up to 80% of ambient NO_2 in cities.[11,14]

Despite the accumulating epidemiological evidence, the burden of paediatric asthma incidence attributable to TRAP exposure remains poorly quantified and has not been included in previous global burden of disease studies.[15,16] In a study published in 2018,[6] Anenberg and colleagues estimated that global asthma incidence attributable to anthropogenic NO_2 and $PM_{2·5}$ might cause about 1·7 million disability-adjusted life-years (DALYs, ie, years of healthy life lost) among children in 2015, with about 97% of this burden due to $PM_{2·5}$. However, this assessment relied on satellite-derived NO_2 concentrations with a spatial resolution of approximately 10×10 km, which likely underestimated the effects of NO_2 for several reasons. First, the mid-afternoon satellite overpass time captures NO_2 concentration at a minimum in its diurnal cycle. Second, given that NO_2 concentrations decline to urban background levels at a distance greater than 300–500 m from major roadways and that intra-urban variation might be more strongly associated with exposure and asthma development than urban–rural variation, the spatial resolution of the satellite data was too coarse.[3,17] An assessment[18] done with a spatial resolution of 100×100 m in a major city in the UK estimated that 18–24% of all annual paediatric asthma incidence might be attributable to ambient NO_2. Because TRAP emissions are ubiquitous, the global burden is likely to be substantial, especially within densely populated urban areas.

In this study, we combined global datasets of NO_2 concentrations, population, and asthma incidence with relative risks drawn from a multinational epidemiological meta-analysis[5] to estimate the annual number of new paediatric asthma cases attributable to ambient NO_2 at a spatial resolution of 250×250 m. We focused on NO_2 because it is a widely used proxy of TRAP and because the evidence for association with paediatric asthma incidence is most robust for TRAP-derived NO_2.

Methods

Population and demographics

We used the 2015 Global Human Settlement population grid (GHS-POP) from the European Commission's Joint Research Centre, which provides population counts for 1975, 1990, 2000, and 2015 at a spatial resolution of 250×250 m, the finest resolution available with global coverage.[19] GHS-POP disaggregates residential population estimates from the Center for International Earth Science Information Network's Gridded Population of the World, version 4 (GPWv4), by use of the distribution and density of built-up areas derived from satellite imaging. To estimate the paediatric population, we calculated age group fractions (1–4, 5–9, 10–14, and 15–18 years) by use of the gridded GPWv4 and the Basic Demographic Characteristics (version 4.10) for 2010, the latest year available.[20] These outputs were then regridded from their original 30 arc-second resolution to 250×250 m and applied to the GHS-POP population estimates. Figure 1A shows national estimates of paediatric population size.

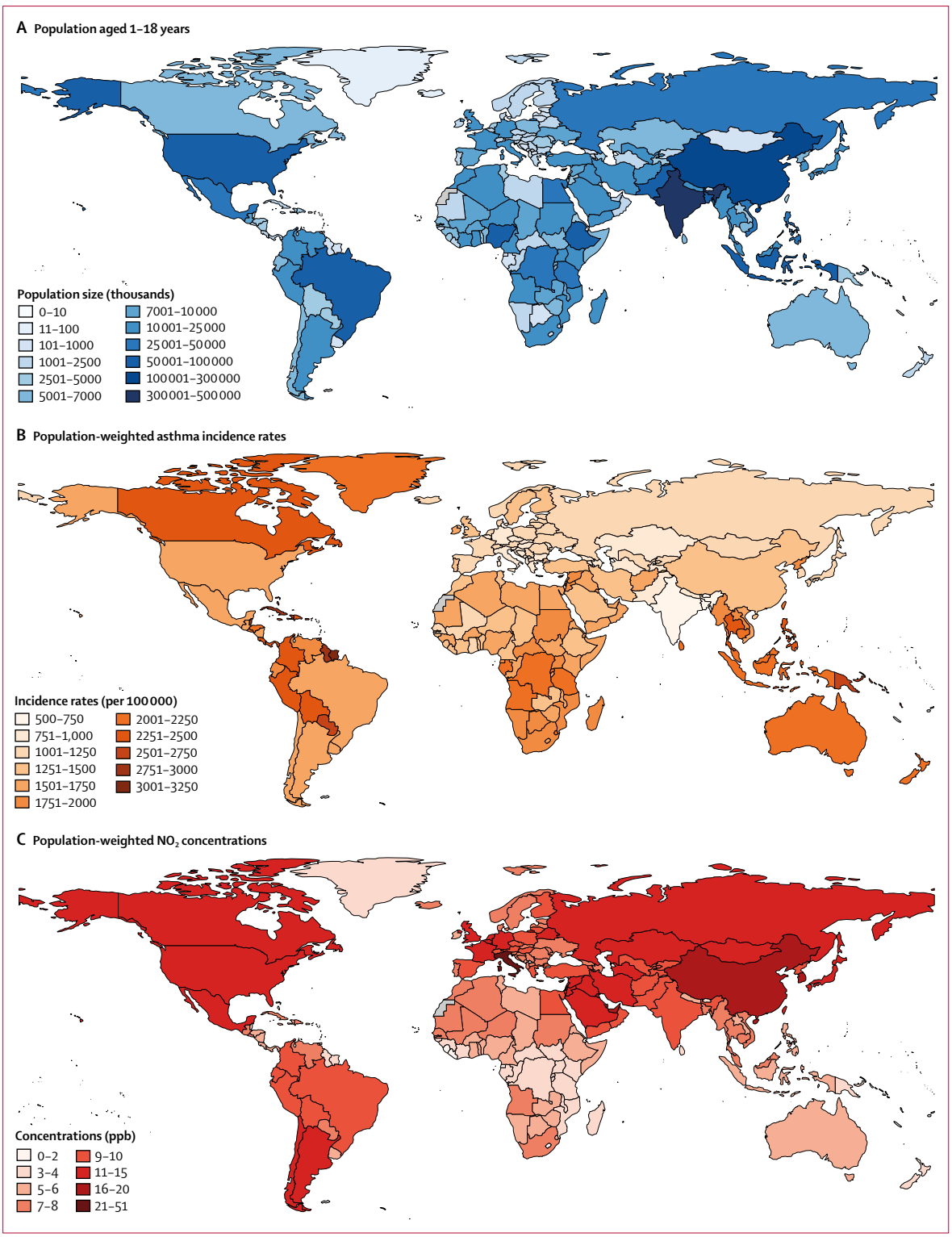

Figure 1: **National estimates of population aged 1–18 years (A), population-weighted annual asthma incidence rates (B), and population-weighted annual average nitrogen dioxide (NO_2) concentrations (C)**

(B) Population-weighted averages were calculated from the country-specific and age-group-specific rates. (C) Concentrations are weighted by the size of the population aged 1–18 years of each country. ppb=parts per billion.

Baseline asthma incidence

We obtained 2015 country-specific and age-group-specific asthma incidence rates from the Institute for Health Metrics and Evaluation (IHME) for 194 countries.[21] We found that most national asthma incidence rates did not change by more than 5% between 2010–12 and 2015 and, therefore, we chose 2015 to match the GHS-POP dataset. The definition of asthma was a reported diagnosis by a physician, with wheezing in the preceding 12 months. Figure 1B shows national asthma incidence rates standardised across the population aged 1–18 years. Additional details on the IHME incidence rates and methods for approximating DALYs are in the appendix.

Concentration-response function

Anenberg and colleagues[6] did a literature review to identify meta-analyses of epidemiological studies on air pollution and asthma, four of which reported paediatric asthma incidence attributable to TRAP-related NO_2 (appendix). These meta-analyses pooled results from individual studies in different countries to derive relative risk (RR) estimates that could be generally representative of the global population. We used the same search criteria as Anenberg and colleagues[6] (appendix) and found no additional meta-analyses published more recently. In this study, we derived concentration response functions (CRFs) from RRs reported by Khreis and colleagues,[5] one of the meta-analyses identified in the search. By comparison with the other three meta-analyses, Khreis and colleagues reviewed the largest number of studies, which included all but one of those considered in the other meta-analyses: 20 studies from Europe, 11 from North America, five from Japan, three from China, one from South Korea, and one from Taiwan, totalling 41 studies; although there was variation in the RRs reported in these studies, no regional heterogeneity was apparent. The meta-analysis[5] reported an overall random-effects RR of 1·26 per 10 parts per billion (ppb) TRAP-related NO_2 (95% uncertainty interval [UI] 1·10–1·37). This UI encompassed the central RR estimates reported in the other three meta-analyses (appendix).

Available evidence is insufficient to establish whether a low-concentration threshold exists, below which there is no risk of paediatric asthma development, and whether the association is linear or non-linear. In this study, we assumed a log-linear relationship between NO_2 concentration and outcome, as Khreis and colleagues did.[5] We applied a counterfactual concentration of 2 ppb, the 5th percentile of the minimum exposure concentrations reported in the individual studies considered by Khreis and colleagues.[5] This approach assumes that long-term exposure to NO_2 less than 2 ppb confers no excess risk of incident asthma in children. As a sensitivity test, we also assumed counterfactual concentrations of 0 ppb and 5 ppb, the 25th percentile of the minimum exposure concentrations reported (appendix).

Ambient NO_2 concentrations

We used a dataset of surface NO_2 concentrations developed by Larkin and colleagues,[22] which is, to date, the only global dataset able to resolve near-roadway concentrations at a spatial resolution of 100×100 m, for 2010–12 annual average concentrations. Larkin and colleagues used land-use regression modelling, an empirical method that combines ground-based air pollution measurements (from 5220 air monitors in 58 countries) with satellite-derived pollutant estimates and other geospatial variables to predict surface concentrations. The strongest predictors of these were major roads within 100 m and satellite-derived NO_2 concentrations. The land-use regression model captured 54% of global NO_2 variation with a mean absolute error of 3·7 ppb. On a continental level, this model varied between capturing 31% (Africa) to 63% (South America) of regional variation, with mean absolute errors ranging from 2·3 ppb (Africa) to 4·4 ppb (North America). The model also generated within-city spatial patterns and concentrations similar to other land-use regression models created for specific cities. Concentrations ranged between 0 ppb and 72 ppb (we estimated that about 0·5% of the global population lived in areas with 0 ppb). Urban–rural and intra-urban concentration gradients for three major cities are shown in the appendix. By comparison, the surface NO_2 concentration dataset used by Anenberg and colleagues[6] had a spatial resolution of 0·1°×0·1° (roughly 10×10 km), with values ranging between 0 ppb and 17·5 ppb. This dataset was derived from column retrievals from the Ozone Monitoring Instrument on board the US National Aeronautics and Space Administration's Aura satellite.[23]

We regridded and reprojected the output from Larkin and colleagues[22] to match the resolution and projection of the population dataset at 250×250 m, by use of the Geospatial Data Abstraction Library. Although some very fine-scale features were lost at this coarser scale, intra-city gradients such as those occurring near major roadways could still be captured at 250 m (appendix). Figure 1C shows national population-weighted NO_2 concentrations.

Health impact function

Following the example of Anenberg and colleagues,[6] we applied methods typically used to assess premature mortality attributable to air pollution to estimate the number of new paediatric asthma cases attributable to NO_2 pollution annually,[15,24] by use of NO_2 data (2010–12 annual average) and population data (2015) that were as recent and as close in time to each other as possible, and spatially resolved below 250 m. The health impact function is:

$$\text{Burden} = Inc_{c,a} \times \sum_{i,j} Pop_{i,j,a} \times \left(1 - e^{-\beta x_{i,j}}\right)$$

where *Inc* is the asthma incidence for country *c* and age group *a* (1–4, 5–9, 10–14, and 15–18 years), *Pop* is the gridded population for age group *a*, β is the concentration-response factor (from the meta-analysis of epidemiological studies), and *X* is the gridded annual average NO_2 concentration. We applied

$$Pop_{i,j,a} \times \left(1 - e^{-\beta X_{i,j}}\right)$$

in each 250×250 m grid cell (*i,j*) globally before summing by national or urban extents. We then multiplied these aggregated sums by the relevant national asthma incidence rates, and provided results for 21 regions, 194 countries, and 125 major cities.

Region, country, and city aggregation

We grouped countries into 21 regions or seven super-regions, according to IHME specifications based on epidemiological similarity and geographical closeness (appendix). Results were aggregated by country by use of the GPWv4 National Identifier Grid.[25] Defining city boundaries is challenging because no universal definition exists.[26] We used a globally consistent definition of urbanisation from the Global Human Settlement 1×1 km grid (GHS-SMOD), for 2015. Urban centres were defined as any contiguous cells with 50 000 or more people and a population density of 1500 or more inhabitants per km² or a density of built-up higher than 50% per grid cell.[27] By combining GHS-SMOD with GHS-POP, we selected the 125 most populous urban centres (population size >3·5 million people). Given that these urban centres do not necessarily match administrative boundaries and sometimes group together multiple neighbouring cities (appendix), we reported city-level results in units of cases per 100 000 children and percentage of total incidence.

Uncertainties in input variables of the health impact function

Although each input variable is uncertain, our results are accompanied by UIs derived from those of the RR, given that this error is well constrained. We also did a sensitivity analysis to compare the influence of uncertainties in the RR, NO_2 concentrations, and asthma incidence rates (uncertainties in the GHS-POP population dataset were not available; appendix).

Role of the funding source

The funder of the study had no role in study design, data collection, data analysis, data interpretation, or writing of the report. PA and SCA had full access to all the data in the study and had final responsibility for the decision to submit for publication.

Results

Globally, we estimated that ambient NO_2 might be associated with 4·0 million (95% UI 1·8–5·2) new paediatric asthma cases annually, accounting for 13% (95% UI 5·8–16) of global incidence (table). The mean burden of new cases associated with ambient NO_2 translates to approximately 730 000 DALYs per year (appendix). We estimated that about 97% of children lived and about 92% of NO_2-attributable paediatric asthma incidence occurred in areas with annual average NO_2 concentrations lower than the WHO guideline of 21 ppb.

Regionally, the largest burden of new asthma cases associated with NO_2 exposure per 100 000 children per year was estimated for Andean Latin America, followed by high-income North America and high-income Asia Pacific (table; appendix). The largest percentage of regional paediatric asthma incidence attributable to NO_2 pollution was estimated for high-income Asia Pacific, followed by east Asia and high-income North America, southern Latin America, and western Europe (table). Eastern sub-Saharan Africa was estimated to have the

	New asthma cases due to NO_2 exposure per year, thousands (95% UI)	New asthma cases due to NO_2 exposure per year, per 100 000 children (95% UI)	New asthma cases due to NO_2 exposure per year, % of total incidence (95% UI)
High income			
Australasia	12 (5·2–15)	170 (77–230)	8·7% (3·8–11)
High-income Asia Pacific	97 (46–120)	300 (140–370)	25% (12–32)
High-income North America	270 (120–340)	310 (140–400)	19% (8·5–24)
Southern Latin America	56 (26–72)	290 (130–370)	18% (8·4–23)
Western Europe	150 (70–200)	190 (85–240)	17% (7·8–22)
Latin America and Caribbean			
Andean Latin America	73 (33–94)	340 (150–440)	15% (6·7–19)
Caribbean	39 (17–51)	280 (120–360)	10% (4·4–13)
Central Latin America	240 (110–310)	260 (120–330)	15% (6·7–19)
Tropical Latin America	150 (66–190)	230 (100–290)	13% (5·8–17)
Sub-Saharan Africa			
Central sub-Saharan Africa	61 (27–79)	110 (47–140)	5·1% (2·3–6·7)
Eastern sub-Saharan Africa	150 (63–190)	76 (33–100)	4·4% (1·9–5·9)
Southern sub-Saharan Africa	46 (20–60)	160 (69–200)	8·6% (3·8–11)
Western sub-Saharan Africa	210 (92–280)	110 (49–150)	7·6% (3·3–9·9)
North Africa and Middle East	570 (260–730)	270 (120–350)	17% (7·6–21)
South Asia	520 (230–680)	82 (37–110)	14% (6·3–18)
Southeast Asia, east Asia, and Oceania			
East Asia	800 (370–1000)	260 (120–340)	19% (8·9–25)
Oceania	3·1 (1·4–4·1)	82 (36–110)	3·1% (1·4–4·1)
Southeast Asia	440 (200–570)	200 (89–260)	9·4% (4·2–12)
Central Europe, eastern Europe, and central Asia			
Central Asia	46 (21–60)	160 (70–200)	16% (7·0–20)
Central Europe	29 (13–38)	130 (60–170)	14% (6·1–18)
Eastern Europe	68 (31–88)	180 (80–230)	17% (7·6–21)
Global	4000 (1800–5200)	170 (77–220)	13% (5·8–16)

95% uncertainty intervals (UI) reflect uncertainties in the relative risk estimates of childhood asthma incidence attributable to traffic-related NO_2 pollution. Countries are grouped into regions according to the Institute for Health Metrics and Evaluation specification (appendix). Numbers are rounded to two significant figures.

Table: **Annual number and percentage of new asthma cases attributable to ambient nitrogen dioxide (NO_2) exposure for children aged 1–18 years**

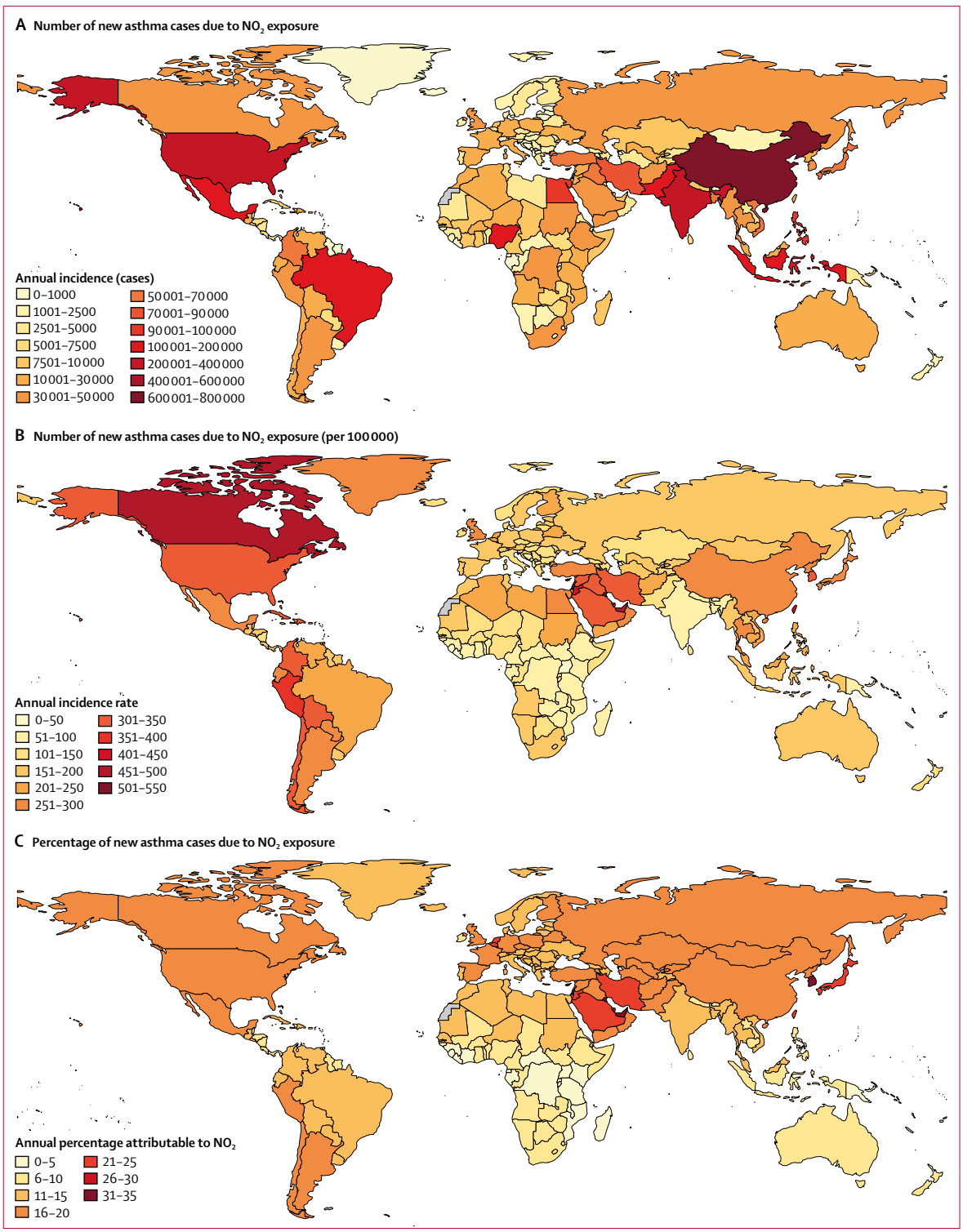

Figure 2: **National annual estimates of number of new asthma cases (A), number of new asthma cases per 100 000 children (B), and percentage of new asthma cases attributable to ambient nitrogen dioxide (NO_2) exposure for children aged 1–18 years**

The values shown are derived using the central mean relative risk estimate and assuming a counterfactual NO_2 concentration of 2 parts per billion.

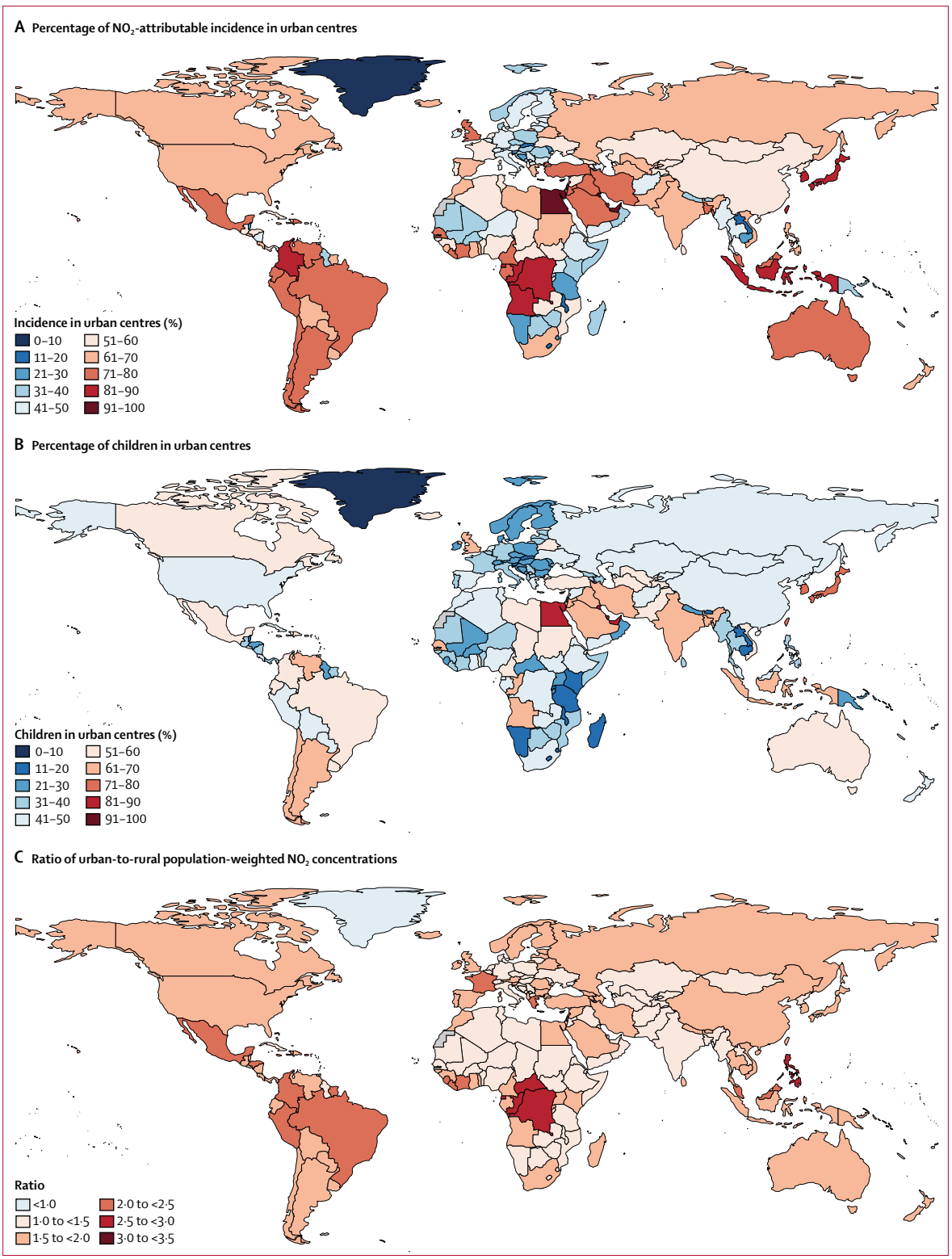

Figure 3: **National annual estimates of percentage of nitrogen dioxide (NO_2)-attributable paediatric asthma incidence occurring in urban centres (A), percentage of children living in urban centres (B), and ratio of population-weighted NO_2 concentration in urban centres relative to non-urban areas (C)**
Urban centres are defined as any contiguous cells with 50 000 or more people and a population density of 1500 or more inhabitants per km² or a density of built-up greater than 50% per grid cell, following the Global Human Settlement classification.

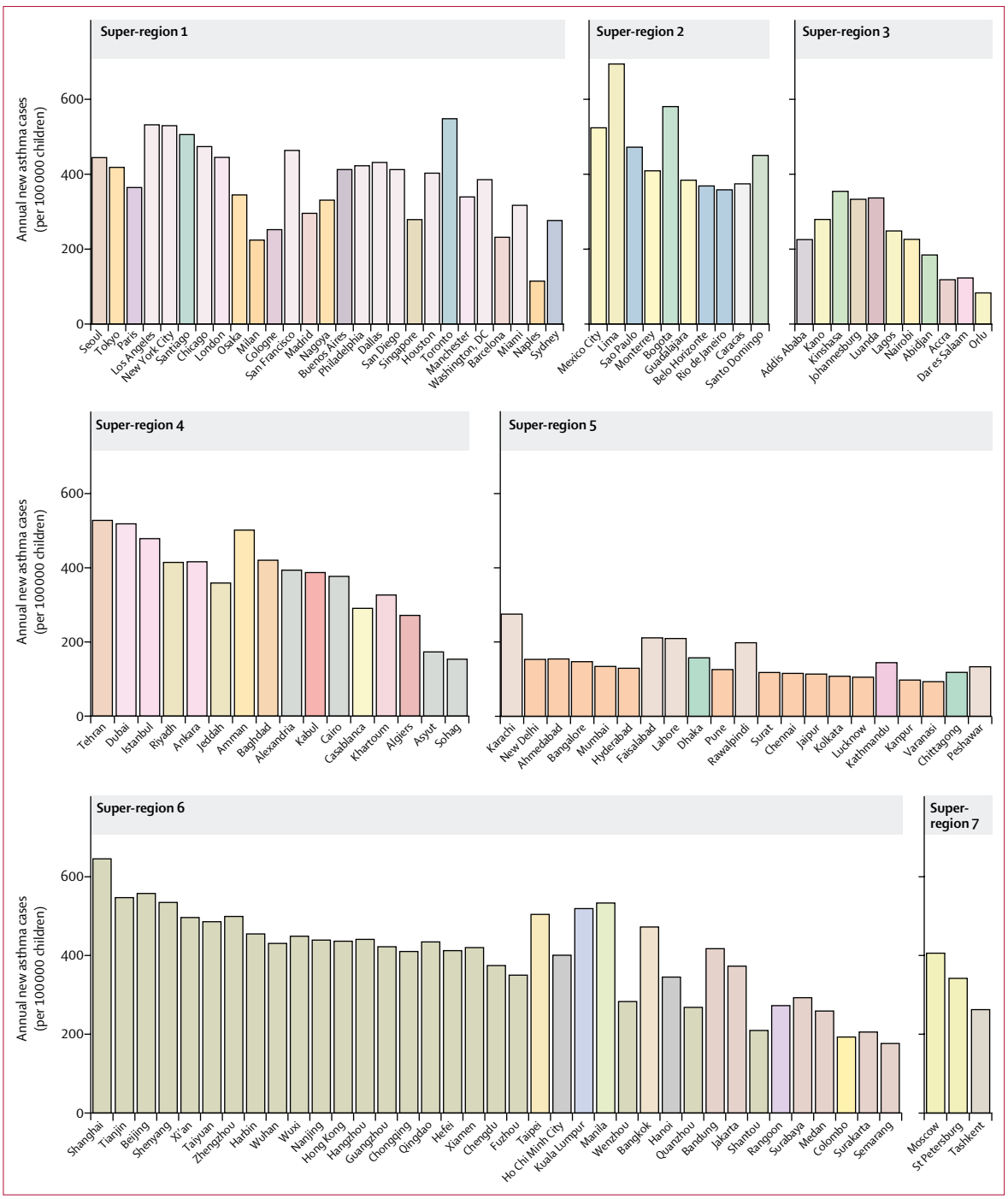

Figure 4: **Annual number of new asthma cases per 100 000 children attributable to ambient nitrogen dioxide (NO_2) exposure for children aged 1–18 years**
Number of new paediatric asthma cases attributable to NO_2 exposure in 125 major cities, grouped into seven super-regions: high income (1); Latin America and Caribbean (2); sub-Saharan Africa (3); north Africa and Middle East (4); south Asia (5); southeast Asia, east Asia, and Oceania (6); and central Europe, eastern Europe, and central Asia (7). Within a super-region, cities were ranked in decreasing order of paediatric population-weighted NO_2 concentrations and coloured by country. The values shown were derived with use of the central mean relative risk estimate and assuming a counterfactual NO_2 concentration of 2 parts per billion. In some cases, an urban centre identified in the Global Human Settlement 1×1 km grid spans multiple cities (see appendix for full urban cluster names).

lowest incidence of new asthma cases attributable to NO_2 exposure per 100 000 children, whereas Oceania had the lowest percentage of incidence attributable to NO_2 (table).

The largest national burdens of new asthma cases attributable to NO_2 exposure were estimated for China (760 000 new cases per year, 95% UI 350 000–970 000),

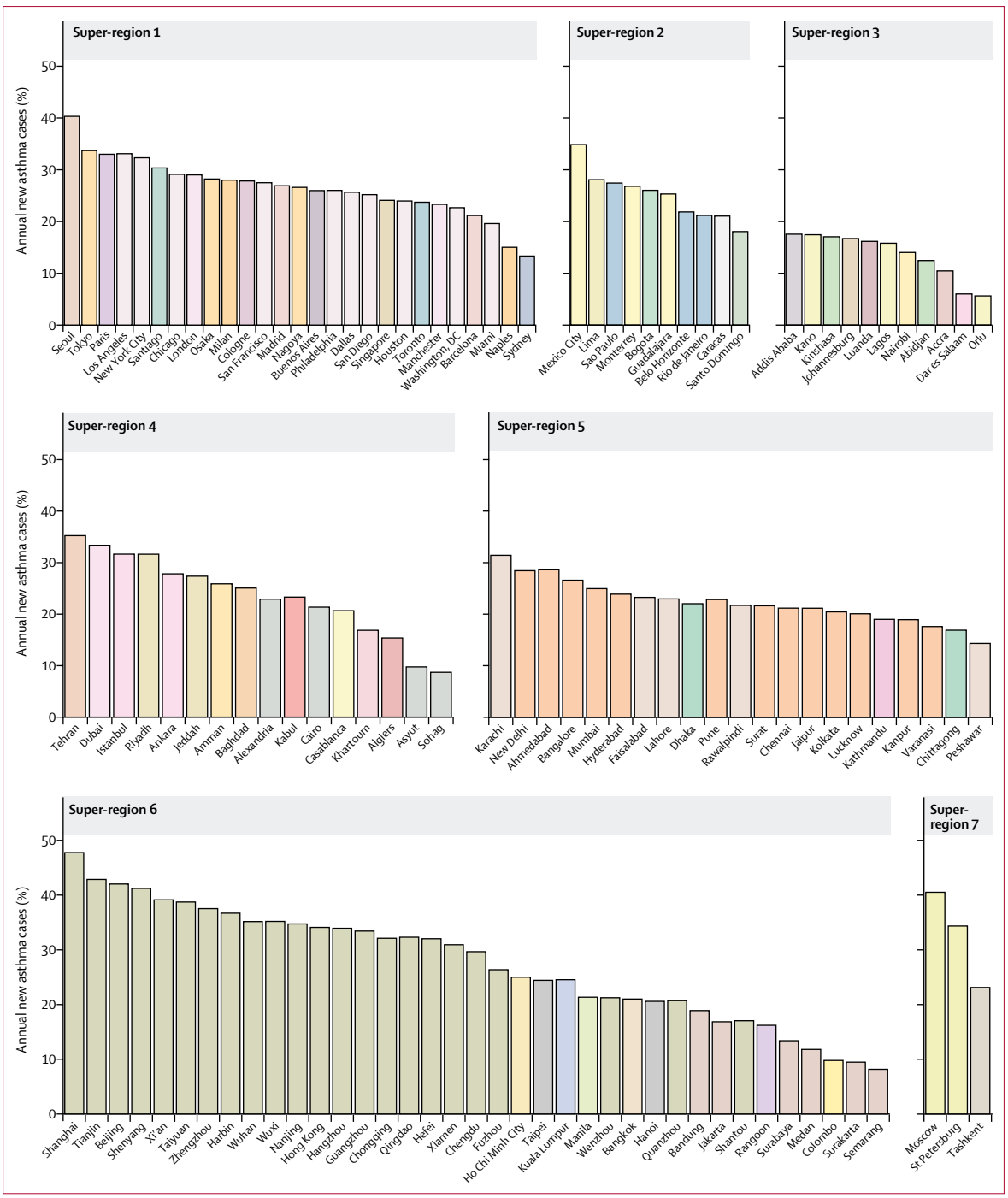

***Figure 5*: Annual percentage of new asthma cases attributable to ambient nitrogen dioxide (NO_2) exposure for children aged 1–18 years**
Percentage of new paediatric asthma cases attributable to NO_2 exposure in 125 major cities, grouped into seven super-regions: high income (1); Latin America and Caribbean (2); sub-Saharan Africa (3); north Africa and Middle East (4); south Asia (5); southeast Asia, east Asia, and Oceania (6); and central Europe, eastern Europe, and central Asia (7). Within a super-region, cities were ranked in decreasing order of paediatric population-weighted NO_2 concentrations and coloured by country. The values shown were derived with use of the central mean relative risk estimate and assuming a counterfactual NO_2 concentration of 2 parts per billion. In some cases, an urban centre identified in the Global Human Settlement 1×1 km grid spans multiple cities (see appendix for full urban cluster names).

India (350 000, 160 000–450 000), the USA (240 000, 110 000–300 000), Indonesia (160 000, 72 000–210 000), and Brazil (140 000, 63 000–180 000; figure 2A, appendix). Of all countries, China had the second largest paediatric population and third highest population-weighted NO_2 concentrations (figure 1). India, despite having the lowest

paediatric asthma incidence rate, had the largest paediatric population. Although the USA, Indonesia, and Brazil had similar paediatric population sizes, the USA had the highest population-weighted NO_2 concentrations and Indonesia had the highest asthma incidence rate among these three countries. The largest national burden per 100 000 children per year was estimated for Kuwait (550 cases per year, 95% UI 260–690), followed by the United Arab Emirates (460, 220–580), Canada (450, 210–580), Taiwan (420, 190–540), and Qatar (410, 200–520; figure 2B) due to high asthma incidence rates, high population-weighted urban NO_2 concentrations, or both. Of 194 countries assessed, Canada had the 34th highest paediatric asthma incidence rate—the highest among high-income nations. Regarding the percentage of asthma incidence attributable to NO_2 exposure, we estimated values exceeding 15% for 48 countries (figure 2C). The highest percentages of asthma incidence attributable to NO_2 were estimated for South Korea (31%, 95% UI 15–38), United Arab Emirates (30%, 14–38), Kuwait (30%, 14–38), and Qatar (30%, 14–37).

We estimated that 64% of paediatric asthma incidence attributable to NO_2 occurred in urban centres globally. This percentage increased to 90% if surrounding sub-urban areas were also considered (GHS-SMOD's so-called low-density clusters). On a national level, the percentage of paediatric asthma incidence attributable to NO_2 occurring in urban centres exceeded 50% in 108 countries (figure 3, appendix), reflecting the distribution of children living in urban areas and the prevalence of high NO_2 concentrations found in urban centres. Generally, national asthma incidence rates were highest in the youngest age group (1–4 years) and decreased with increasing age. This effect dwarfed the age group variations in population size, resulting in the largest asthma burdens attributable to NO_2 being estimated for children aged 1–4 years, both in total and per 100 000 children, in all but one country (Moldova; appendix). Regarding the influence of uncertainties in the input variables, we found that asthma incidence rates had the least influence, given that their UIs were small. UIs resulting from those of RRs and from NO_2 concentrations were generally within the same order of magnitude (appendix).

Of the 125 major cities we investigated, the largest burdens of paediatric asthma incidence attributable to NO_2 exposure per 100 000 children were estimated for Lima, Peru (690 cases per year, 95% UI 330–870); Shanghai, China (650, 340–770); Bogota, Colombia (580, 270–730); Beijing, China (560, 280–680); and Toronto, Canada (550, 250–700; figure 4, appendix). The large burdens estimated for Chinese cities were primarily driven by high population-weighted NO_2 concentrations (28–33 ppb). By contrast, Lima, Bogota, and Toronto had medium NO_2 concentrations (14–17 ppb), but had among the highest national paediatric asthma incidence rates, especially for children aged 1–4 years, in the 54 countries where the 125 cities are located. The lowest population-standardised burdens were found in Orlu, Nigeria (83 cases per year, 95% UI 36–110), and in four cities in India (Varanasi, 88 [40–110]; Kanpur, 92 [42–120]; Lucknow, 99 [45–130]; and Kolkata, 100 [47–130]; figure 4, appendix). India had the lowest asthma incidence rate among all countries, whereas Orlu had the lowest population-weighted NO_2 concentration (5 ppb). The percentage of new asthma cases attributable to NO_2 pollution by city ranged from 5·6% (95% UI 2·4–7·4) in Orlu, Nigeria, to 48% (25–57) in Shanghai, China, and primarily reflected the variations in NO_2 exposures within each region (figure 5). These percentages exceeded 20% in 92 cities and exceeded 30% in 32 cities (figure 5, appendix). The ten largest contributions were estimated for eight cities in China (Shanghai, Tianjin, Beijing, Shenyang, Xi'an, Taiyuan, Zhengzhou, and Harbin), for Moscow (Russia), and for Seoul (South Korea; figure 5, appendix). All these cities had high urban NO_2 concentrations. The meta-analysis from which the RRs were drawn included three epidemiological studies done in China.

Discussion

This study provides the first global estimate of the burden of paediatric asthma incidence attributable to ambient NO_2 at a spatial resolution fine enough to resolve intra-urban and near-roadway exposure gradients, for 194 countries and 125 major cities. We estimated that, each year, 4·0 million (95% UI 1·8–5·2) new cases of paediatric asthma might be attributable to NO_2 pollution, accounting for 13% (5·8–16) of global incidence; 48 of 194 countries had percentages greater than 15% of national incidence. The city-level percentages ranged between 6% and 48%, with 92 of 125 cities exceeding 20%. The 2015 Global Burden of Disease study[21] estimated that smoking and occupational asthmagens could account for 16·5% of the global asthma prevalence for all ages in 2015. Although the burden of premature mortality attributable to ambient $PM_{2·5}$ pollution is generally greater in low-income and middle-income countries because of high exposures,[15] the effects of NO_2 pollution on paediatric asthma incidence appear to be less differentiated by level of development. Many high-income countries have high NO_2 exposures, especially those in North America, western Europe, and Asia Pacific. In Canada, this problem is also exacerbated by high paediatric asthma incidence rates (appendix).

Because transportation can contribute up to 80% of ambient NO_2 in cities and is an important driver of increasing greenhouse gas emissions globally,[14,28] we also explored whether there were associations between carbon dioxide (CO_2) emissions and NO_2 exposure, to highlight potential co-benefits of exposure-mitigation policies. We found that, in general, countries and cities with higher CO_2 emissions tended to have higher paediatric NO_2 exposures and larger burdens of asthma incidence attributable to ambient NO_2 (appendix).

Anenberg and colleagues[6] have estimated the global burden of asthma incidence attributable to anthropogenic NO_2 for children aged 0–17 years, relying on satellite-derived NO_2 concentrations, from the Ozone Monitoring Instrument, at a resolution of roughly 10×10 km. The authors suggested that they likely underestimated actual exposures because the satellite's mid-afternoon overpass time coincides with the minimum concentration in diurnal NO_2 variation and because near-roadway concentrations were not resolved. Indeed, with use of the same RR drawn from Khreis and colleagues,[5] but with different population data, their estimated global burden of 1·3 million new asthma cases per year attributable to NO_2 is about 3·1 times smaller than our estimate assuming a counterfactual concentration of 2 ppb (and about 1·7 times smaller than our estimate assuming a counterfactual concentration of 5 ppb). In another study,[18] published in 2018, Khreis and colleagues quantified the annual paediatric asthma incidence attributable to air pollution in Bradford, UK, by use of concentration estimates at 100×100 m resolution and assuming no low concentration threshold. By use of ambient NO_2 concentrations modelled by land-use regression, Khreis and colleagues estimated that 24% of annual paediatric asthma cases might be attributable to NO_2 exposure in 2009 (with an annual mean NO_2 concentration of 12 ppb). This matches our equivalent estimate (assuming a counterfactual of 0 ppb) of 28% for the Leeds–Bradford metropolitan area, which had annual mean NO_2 concentrations of 13 ppb during 2010–12. Estimates assuming a counterfactual concentration of 2 ppb were 23%, whereas those assuming 5 ppb were 17% (data not shown).

Several important limitations and uncertainties exist in our approach. First, the epidemiological evidence considered by Khreis and colleagues[5] and the ground-based NO_2 monitoring data used in the global land-use regression model for NO_2 developed by Larkin and colleagues[22] are mainly available only for North America, Europe, and east Asia. These limitations in the global representation of the outcome measure and of the exposure characterisation upon which we relied consequently apply to our estimates. Additionally, because most ground-based NO_2 monitors are in urban areas, the global land-use regression model might overestimate concentrations in rural areas. However, this is unlikely to add appreciable bias because rural populations are sparse. Available epidemiological studies have also been done within a range (about 1–50 ppb) that approximately spans global exposures (0–72 ppb).

A second limitation is that NO_2 concentrations used in this study represent the 2010–12 annual average, whereas the population and asthma incidence rates are 2015 estimates. Duncan and colleagues[29] found that between 2005 and 2014, there have been substantial trends in urban NO_2 concentrations worldwide, with general decreases in US and European cities and increases in Asia, although complex spatial heterogeneity exists. Future assessments could apply these trends to the NO_2 land-use regression dataset to estimate effects in other years.

Third, we relied on national paediatric asthma incidence rates in our analysis, but subnational variations most likely exist, especially between urban and rural populations. Additionally, although the IHME incidence rates were derived from prevalence data covering 121 countries and all 21 regions,[21] the definition of asthma based on physician diagnosis might underestimate the effects of vehicular emissions on asthma in low-income and middle-income countries because of low health-care access or the neglect of subclinical symptoms that might not manifest in a diagnosis. Fourth, uncertainties remain in the shape of the CRF of paediatric asthma incidence and NO_2 exposure. In this study, we assumed a log-linear relationship and a low-concentration threshold of 2 ppb. We also assumed a causal relationship between NO_2 exposure and asthma incidence and used a CRF derived from single-pollutant epidemiological models (because multipollutant models were not available). The evidence so far suggests that associations with asthma incidence are more robust for NO_2 than for other air pollutants and that NO_2 is better than $PM_{2·5}$ for representing near-roadway variability of the TRAP mixture.[30,31] However, it is possible that NO_2 is a proxy for other putative agents in the TRAP mixture, that the reported associations are sensitive to control for co-pollutants, or both. All these uncertainties mean that our NO_2-attributable asthma estimates might be overestimated or underestimated.

Our analysis and characterisation of uncertainties can consequently be improved by future studies aiming to resolve the limitations described. The availability of global NO_2 concentration and population datasets that are up to date and have even finer temporal and spatial resolutions than those of the datasets used in this study will be particularly valuable. In this study, we did not isolate traffic-specific contributions to ambient NO_2 concentrations, but this approach is more consistent with existing epidemiological studies, the majority of which also relied on NO_2 exposures derived from land-use regression without isolating the contribution of traffic emissions.[5] Isolating the role of TRAP can help to constrain estimates of the portion of total asthma incidence that could be avoided by targeting this emission source. Additionally, it would be useful for future epidemiological studies to identify the putative agents within the TRAP mixture and target understudied populations, especially in Africa and central and southeast Asia.

Despite substantial decreases in NO_2 concentrations over the past decade in large areas of the USA and western Europe,[29] our findings suggest that existing levels of ambient NO_2 pollution are a substantial risk factor for paediatric asthma incidence in both developed and developing countries, especially in urban areas. In fact, our findings suggest that the adequacy of the WHO

guideline for annual average NO_2 concentrations might need to be revisited. We also found that countries and cities with higher CO_2 emissions from fossil fuel combustion tend to have higher NO_2 exposures, providing further support that alignment of policy initiatives to mitigate air pollution and climate change can have multiple public health benefits.[32,33] Traffic emissions should be a target for exposure-mitigation strategies.

Contributors

SCA and MB conceived the project idea. SCA and PA designed the analysis methods. PH and MB contributed to the development of the land-use regression NO_2 dataset used in this analysis. PA did the analysis and had primary responsibility for writing the manuscript, to which all authors contributed.

Declaration of interests

SCA provided research consulting services on separate projects for the International Council on Clean Transportation and the Health Effects Institute within the 36 months during and before the work reported in this article. PA, MB, and PH declare no competing interests.

Acknowledgments

Funding was provided by the George Washington University. We thank all the data providers for making their data publicly available. Baseline disease rates were provided by the Institute of Health Metrics and Evaluation. Global Human Settlement (GHS) population and urban extents were provided by the Joint Research Centre of the European Commission. Open-source Data Inventory for Anthropogenic CO_2 (ODIAC) emissions dataset was provided by Tomohiro Oda of Colorado State University (Fort Collins, CO, USA) and Global Monitoring Division, US National Oceanic and Atmospheric Administration's Earth System Research Laboratory (Boulder, CO, USA). The ODIAC project is supported by Greenhouse Gas Observing Satellite project, National Institute for Environmental Studies, Japan. We thank Andrew Larkin for providing the NO_2 dataset and technical advice, Haneen Khreis for helpful discussions on the TRAP-asthma epidemiology, Aneta J Florczyk and Sergio Freire for providing insights into the GHS datasets, and Casey Kalman for research assistance on matching GHS-SMOD urban centre identifiers to city names using ArcGIS.

References

1 WHO. Asthma fact sheet. 2017. http://www.who.int/en/news-room/fact-sheets/detail/asthma (accessed July 24, 2018).

2 Gasana J, Dillikar D, Mendy A, Forno E, Ramos Vieira E. Motor vehicle air pollution and asthma in children: a meta-analysis. *Env Res* 2012; **117:** 36–45.

3 Anderson HR, Favarato G, Atkinson RW. Long-term exposure to air pollution and the incidence of asthma: meta-analysis of cohort studies. *Air Qual Atmos Heal* 2013; **6:** 47–56.

4 Bowatte G, Lodge C, Lowe AJ, et al. The influence of childhood traffic-related air pollution exposure on asthma, allergy and sensitization: a systematic review and a meta-analysis of birth cohort studies. *Allergy* 2014; **70:** 245–56.

5 Khreis H, Kelly C, Tate J, Parslow R, Lucas K, Nieuwenhuijsen M. Exposure to traffic-related air pollution and risk of development of childhood asthma: a systematic review and meta-analysis. *Environ Int* 2017; **100:** 1–31.

6 Anenberg SC, Henze DK, Tinney V, et al. Estimates of the global burden of ambient PM2·5, ozone, and NO_2 on asthma incidence and emergency room visits. *Environ Health Perspect* 2018; **126:** 107004.

7 Guarnieri M, Balmes JR. Outdoor air pollution and asthma. *Lancet* 2014; **383:** 1581–92.

8 MacIntyre EA, Brauer M, Melen E, et al. GSTP1 and TNF gene variants and associations between air pollution and incident childhood asthma: the Traffic, Asthma and Genetics (TAG) study. *Environ Health Perspect* 2014; **122:** 418–24.

9 Khreis H, Nieuwenhuijsen MJ. Traffic-related air pollution and childhood asthma: recent advances and remaining gaps in the exposure assessment methods. *Int J Environ Res Public Health* 2017; **14:** 312.

10 Beckerman B, Jerrett M, Brook JR, Verma DK, Arain MA, Finkelstein MM. Correlation of nitrogen dioxide with other traffic pollutants near a major expressway. *Atmos Environ* 2008; **42:** 275–90.

11 Levy I, Mihele C, Lu G, Narayan J, Brook JR. Evaluating multipollutant exposure and urban air quality: pollutant interrelationships, neighborhood variability, and nitrogen dioxide as a proxy pollutant. *Environ Health Perspect* 2014; **122:** 65–72.

12 Health Canada. Human health risk assessment for ambient nitrogen dioxide. Ottawa: Health Canada, 2016.

13 US Environmental Protection Agency. Integrated science assessment for oxides of nitrogen—health criteria. Research Triangle Park: US Environmental Protection Agency, 2016.

14 Sundvor I, Castell Balaguer N, Viana M, et al. Road traffic's contribution to air quality in European cities—ETC/ACM technical paper 2012/14. Copenhagen: European Topic Centre for Air Pollution and Climate Change Mitigation, 2013.

15 Cohen AJ, Brauer M, Burnett R, et al. Estimates and 25-year trends of the global burden of disease attributable to ambient air pollution: an analysis of data from the Global Burden of Diseases Study 2015. *Lancet* 2017; **389:** 1907–18.

16 Prüss-Üstün A, Wolf J, Corvalán CF, Bos R, Neira MP. Preventing disease through healthy environments: a global assessment of the burden of disease from environmental risks. Geneva: World Health Organization, 2016.

17 Health Effects Institute. Traffic-related air pollution: a critical review of the literature on emissions, exposure, and health effects. Boston: Health Effects Institute, 2010.

18 Khreis H, de Hoogh K, Nieuwenhuijsen MJ. Full-chain health impact assessment of traffic-related air pollution and childhood asthma. *Environ Int* 2018; **114:** 365–75.

19 European Commission Joint Research Centre, Columbia University Center for International Earth Science Information Network. GHS population grid, derived from GPW4, multitemporal (1975, 1990, 2000, 2015). 2015. http://data.europa.eu/89h/jrc-ghsl-ghs_pop_gpw4_globe_r2015a (accessed Feb 20, 2018).

20 Center for International Earth Science Information Network, Columbia University. Gridded Population of the World, version 4 (GPWv4): basic demographic characteristics, revision 10. 2017. http://beta.sedac.ciesin.columbia.edu/data/set/gpw-v4-basic-demographic-characteristics-rev10 (accessed Feb 12, 2018).

21 GBD 2015 Chronic Respiratory Disease Collaborators. Global, regional, and national deaths, prevalence, disability-adjusted life years, and years lived with disability for chronic obstructive pulmonary disease and asthma, 1990–2015: a systematic analysis for the Global Burden of Disease Study 2015. *Lancet Respir Med* 2017; **5:** 691–706.

22 Larkin A, Geddes JA, Martin R V, et al. Global land use regression model for nitrogen dioxide air pollution. *Environ Sci Technol* 2017; **51:** 6957–64.

23 Lamsal LN, Martin R V, van Donkelaar A, et al. Ground-level nitrogen dioxide concentrations inferred from the satellite-borne Ozone Monitoring Instrument. *J Geophys Res Atmos* 2008; **113:** D16.

24 Anenberg SC, Horowitz LW, Tong DQ, West JJ. An estimate of the global burden of anthropogenic ozone and fine particulate matter on premature human mortality using atmospheric modeling. *Environ Health Perspect* 2010; **118:** 1189–95.

25 Center for International Earth Science Information Network, Columbia University. Gridded Population of the World, version 4 (GPWv4): national identifier grid, revision 10. 2017. http://sedac.ciesin.columbia.edu/data/set/gpw-v4-national-identifier-grid-rev10 (accessed April 10, 2018).

26 Uchiyama Y, Mori K. Methods for specifying spatial boundaries of cities in the world: the impacts of delineation methods on city sustainability indices. *Sci Total Environ* 2017; **592:** 345–56.

27 Pesaresi M, Freire S. GHS settlement grid following the REGIO model 2014 in application to GHSL Landsat and CIESIN GPW v4-multitemporal (1975–1990–2000–2015). 2016. http://data.europa.eu/89h/jrc-ghsl-ghs_smod_pop_globe_r2016a (accessed Feb 20, 2018).

28 IPCC. Drivers, trends and mitigation. In: Intergovernmental panel on climate change, ed. Climate change 2014: mitigation of climate change—working group III contribution to the IPCC fifth assessment report. Cambridge: Cambridge University Press, 2015: 351–412.

29 Duncan BN, Lamsal LN, Thompson AM, et al. A space-based, high-resolution view of notable changes in urban NOx pollution around the world (2005–2014). *J Geophys Res Atmos* 2015; **121:** 976–96.

30 Karner AA, Eisinger DS, Niemeier DA. Near-roadway air quality: synthesizing the findings from real-world data. *Environ Sci Technol* 2010; **44:** 5334–44.

31 Cooper MJ, Martin R V, van Donkelaar A, Lamsal L, Brauer M, Brook JR. A satellite-based multi-pollutant index of global air quality. *Environ Sci Technol* 2012; **46:** 8523–24.

32 Anenberg SC, Miller J, Minjares R, et al. Impacts and mitigation of excess diesel-related NOx emissions in 11 major vehicle markets. *Nature* 2017; **545:** 467.

33 West JJ, Smith SJ, Silva RA, et al. Co-benefits of mitigating global greenhouse gas emissions for future air quality and human health. *Nat Clim Chang* 2013; **3:** 885.

THE LANCET
Planetary Health

Supplementary appendix

This appendix formed part of the original submission and has been peer reviewed. We post it as supplied by the authors.

Supplement to: Achakulwisut P, Brauer M, Hystad P, Anenberg SC. Global, national, and urban burdens of paediatric asthma incidence attributable to ambient NO_2 pollution: estimates from global datasets. *Lancet Oncol* 2019; published online April 10. http://dx.doi.org/10.1016/S2542-5196(19)30046-4.

Supplemental text, figures, and tables

S1. Additional methods details

Literature review of concentration-response factor (CRF)

Using the search criteria outlined in Anenberg et al. (2018), we conduct a literature review to identify meta-analyses of epidemiological studies on paediatric asthma incidence associated with traffic-related air pollution (TRAP) exposure, using MEDLINE, PubMed, and Google Scholar. We limited the search to meta-analyses that included individual studies from multiple countries, reported a numerical concentration-response relationship accompanied by an estimate of precision, and were written in English. Based on these criteria, no new study has been published to date (as of March 2018) beyond the four meta-analyses identified by Anenberg et al. (shown in Table S1).

Baseline asthma incidence rates

Country- and age-group-specific asthma incidence rates were obtained from the Institute for Health Metrics and Evaluation's Global Health Data Exchange (IHME GHDx) for 2015, with data available for 195 countries. The definition of asthma was a reported diagnosis by a physician, with wheezing in the past 12 months. National asthma incidence and prevalence rates were estimated using the DisMod MR ("Disease Modeling – Metaregression") 2.1 modeling tool (a Bayesian meta-regression model to estimate age-sex-country specific prevalence from heterogeneous and often sparse data sets; earlier version described by Barendregt et al., 2003) with input data from the WHO Study on Global Aging and Adult Health series, the WHO World Health Survey series, the Belgian Health Interview Survey, and studies carried out as part of the International Study of Asthma and Allergies in Childhood (ISAAC) collaboration, claims data in the U.S., and other sources for individual countries where available [GBD 2015 Chronic Respiratory Disease Collaborators, 2017]. The percentage of geographies (country or in limited cases, subnational administrative regions) with data on asthma rates (65%) was relatively high compared to many other diseases, including ischemic heart disease (51%) and COPD (32%), and cover all 21 IHME world regions. In the absence of data from a particular geography, information from the parent geography was used.

Approximation of Disability-Adjusted Life Years (DALYs)

The outputs from Equation 1 are in units of number of new asthma cases. We convert these to DALYs by assuming that the ratio of NO_2-attributable asthma DALYs to the total asthma DALYs is the same as the ratio of NO_2-attributable asthma cases to the total number of asthma cases for each country and age group. Country- and age-group-specific asthma DALYs were obtained from the IHME GHDx for 2015 (GBD 2015 Chronic Respiratory Disease Collaborators, 2017).

S2. Sensitivity analysis of counterfactual concentration

Under the assumption that there is no low concentration threshold below which excess risk of incidence asthma does not occur, the global burden of NO_2-attributable paediatric asthma incidence is 5·4 (2·4-7·1) million new cases per year, accounting for 17% (7·6-22%) of global incidence. The percentages of new paediatric asthma cases attributable

to NO_2 range between 0-35% at national levels, and between 10-52% at urban levels. Using a more conservative threshold level of 5 ppb (based on the 25th percentile of the minimum exposure levels reported in the epidemiological studies considered by Khreis et al., 2017), the global burden of NO_2-attributable paediatric asthma incidence is 2·3 (1·1-2·9) million new cases per year, accounting for 7·2% (3·4-9·0%) of global incidence. The percentages of new paediatric asthma cases attributable to NO_2 range between 0-24% at national levels, and between 0·6-41% at urban levels. National and urban burdens assuming counterfactual concentrations of 0, 2, and 5 ppb are shown in Tables S5-S6.

S3. Uncertainties in input variables of the health impact function

To account for potential uncertainties in the gridded NO_2 concentrations and country- and age group-specific asthma incidence rates in addition to those in the relative risk, we perform a sensitivity analysis by applying lower, central, and upper estimates of each of these input variables in turn to Equation 1, while keeping the others constant at the central values. Uncertainties in the GHS-POP population dataset are not provided. We assume a counterfactual concentration of 2 ppb in all sensitivity calculations. The lower, central, and upper estimates of each variable are defined as follows:

- Relative risk: the mean random-effects risk estimate and 95% uncertainty interval from meta-analysis of 20 individual epidemiological studies (Khreis et al., 2017).
- Country- and age group-specific asthma incidence rate: the mean and 95% uncertainty interval of the posterior distribution (from 1,000 simulations of the DisMod MR 2.1 model).
- NO_2: Larkin et al. (2017) provided mean absolute errors of the global LUR NO_2 model at the continental level. We approximate the lower and upper estimates of NO_2 concentrations by subtracting or adding the corresponding continental errors to each grid cell, respectively.

Uncertainty intervals in the burden of NO_2-attributable paediatric asthma incidence due to uncertainties in different input variables, summarized over 21 regions, is displayed in Figure S3. Uncertainties in the country- and age group-specific asthma incidence rates have the least influence, given that they are relatively small and that the burden calculated from Equation 1 would scale linearly with changes in the asthma incidence rate but exponentially with changes in the relative risk or NO_2 concentrations. Uncertainty intervals resulting from those in the relative risk and NO_2 concentrations are generally comparable, though in several regions NO_2 can have a much larger impact (e.g., Andean Latin America and Southeast Asia). However, the uncertainties in NO_2 are likely exaggerated here since we applied the continental-level mean absolute errors provided by Larkin et al. (2017) to each relevant grid box. The largest UIs are estimated for Andean Latin America and the Caribbean when uncertainties in the relative risk or surface NO_2 concentrations are considered. The shape of the log-linear CRF (Equation 1) means that changes in the NO_2 concentration or relative risk at lower values result in larger changes in the NO_2-attributable burdens. In general: (1) Average NO_2 concentrations in these two regions are just above our assumed counterfactual concentration of 2ppb (2.8 ppb in the Caribbean and 3.7 ppb in Andean Latin America); and (2) These two regions rank first (Caribbean) and third (Andean Latin America) in terms of highest population-weighted asthma incidence rates. As a result, the

higher sensitivity to changes in the NO_2 concentration or relative risk values are amplified by the high incidence rates in countries located in these two regions.

S4. NO_2-attributable paediatric asthma incidence versus greenhouse gas emissions

Given that transportation is an important driver of increasing greenhouse gas (GHG) emissions globally, we examine whether there are associations between NO_2-attributable paediatric asthma incidence and GHG emissions at national and city levels to identify potential co-benefits of exposure-mitigation policies. Annual mean CO_2 emissions for 2010-2012 are calculated from the satellite-derived 1 km x 1 km Open-source Data Inventory for Anthropogenic CO_2 (ODIAC, v2017) from fossil fuel combustion (Oda et al., 2011), and summed by country or city using the methods described in the main text.

We find statistically significant positive relationships between NO_2-attributable paediatric asthma incidence and CO_2 emissions from fossil fuel combustion in terms of national sums (Figure S5a; $r = 0{\cdot}72$, p = 2e-30) and urban per capita values (Figure S5c; $r = 0{\cdot}56$, p = 2e-11). National per capita values also display a positive but more variable relationship (Figure S6a; $r = 0{\cdot}40$, p = 1e-8). In general, countries and cities with higher CO_2 emissions tend to have higher paediatric population-weighted NO_2 concentrations (Figure S5b,d). Thus, many locations have opportunities to achieve multiple societal benefits by reducing pollution from fossil fuel combustion – in particular, countries and cities located in East Asia, North Africa and Middle East, and High-income North America, Western Europe, and Asia Pacific.

References

1. Anenberg SC, Henze DK, Tinney V, Kinney PL, Raich W, Fann N, et al. Estimates of the Global Burden of Ambient PM2.5, Ozone, and NO2 on Asthma Incidence and Emergency Room Visits. Environ Health Perspect. 2018 Oct 30;126(10):107004.
2. Barendregt JJ, van Oortmarssen GJ, Vos T, Murray CJ. A generic model for the assessment of disease epidemiology: the computational basis of DisMod II. Popul Health Metr. 2003;1(1):4, PMID: 12773212, https://doi.org/10.1186/1478-7954- 1-4.
3. GBD 2015 Chronic Respiratory Disease Collaborators. Global, regional, and national deaths, prevalence, disability-adjusted life years, and years lived with disability for chronic obstructive pulmonary disease and asthma, 1990-2015: a systematic analysis for the Global Burden of Disease Study 2015. Lancet Respir Med. 2017 Sep 1;5(9):691–706.
4. Khreis H, Kelly C, Tate J, Parslow R, Lucas K, Nieuwenhuijsen M. Exposure to traffic-related air pollution and risk of development of childhood asthma: A systematic review and meta-analysis. Environ Int. 2017;100:1–31.
5. Larkin A, Geddes JA, Martin R V, Xiao Q, Liu Y, Marshall JD, et al. Global Land Use Regression Model for Nitrogen Dioxide Air Pollution. Environ Sci Technol. 2017 Jun 20;51(12):6957–64.

6. Oda T, Maksyutov S. A very high-resolution (1 km×1 km) global fossil fuel CO2 emission inventory derived using a point source database and satellite observations of nighttime lights. Atmos Chem Phys. 2011 Jan 18;11(2):543–56.

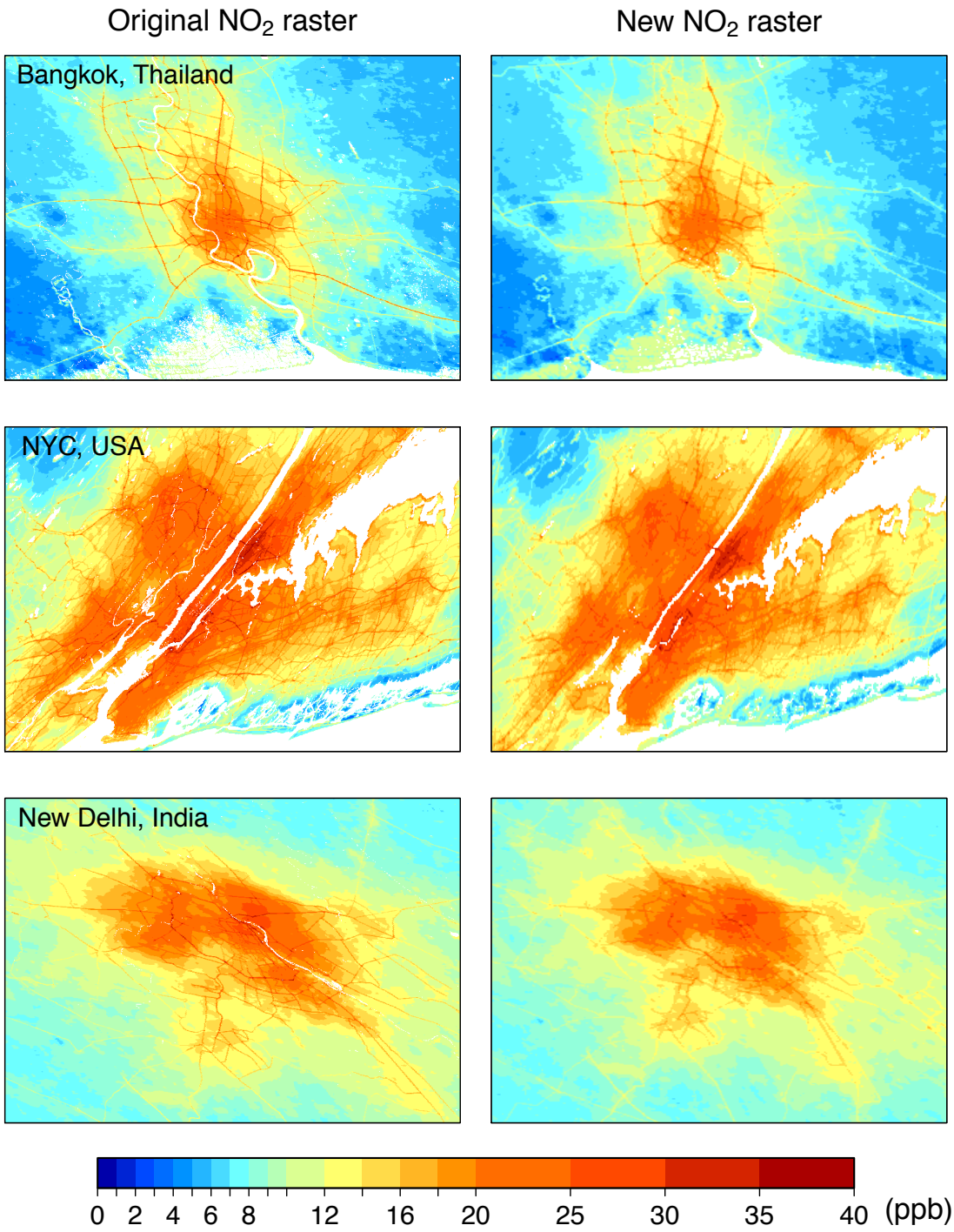

Figure S1. 2010-2012 annual mean NO_2 concentrations (ppb) from Larkin et al. [2017], zoomed into three cities to focus on intra-urban and urban-rural variations. Left panels: original raster at 100 m x 100 m in the Goode homolosine projection. Right panels: regridded and reprojected raster at 250 m x 250 m in the Mollweide projection.

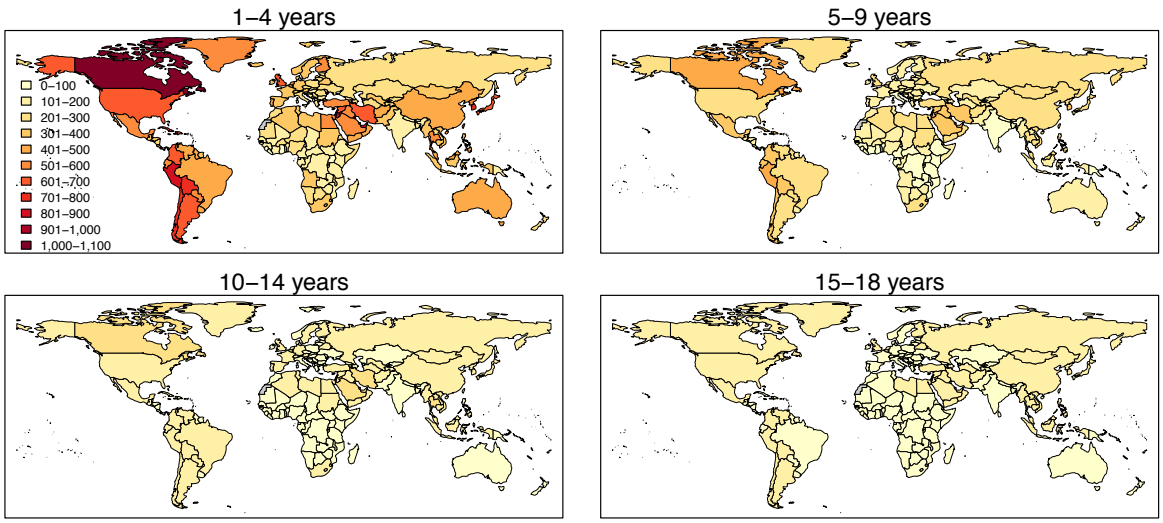

Figure S2. National estimates of annual number of new paediatric asthma cases per 100k attributable to ambient NO_2 exposure by age group (values are standardized by the population size of each age group). The values shown are derived using the central mean relative risk estimate and assuming a counterfactual concentration of 2 ppb.

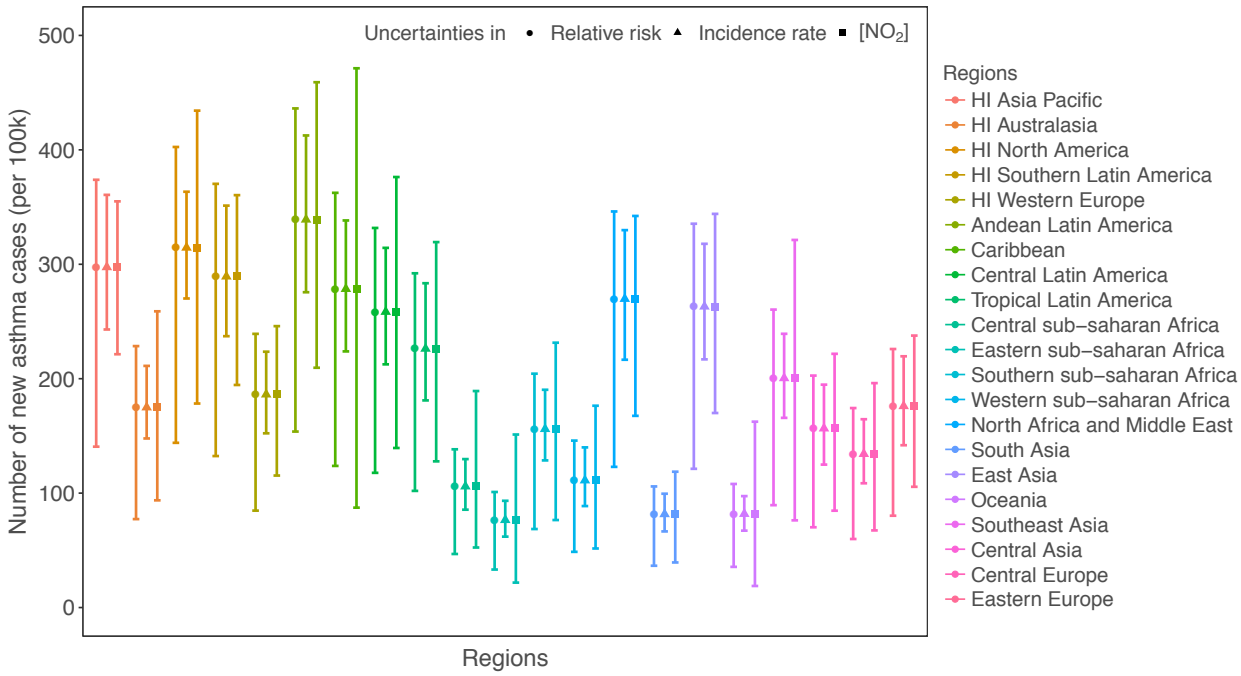

Figure S3. Comparison of uncertainty intervals in estimates of NO_2-attributable paediatric asthma incidence (cases per 100k children), summarized over 21 regions, due to uncertainties in different input variables: relative risk (circle), asthma incidence rate (triangle), and ambient NO_2 concentrations (square). Colors represent different regions. All estimates are derived assuming a counterfactual concentration of 2 ppb.

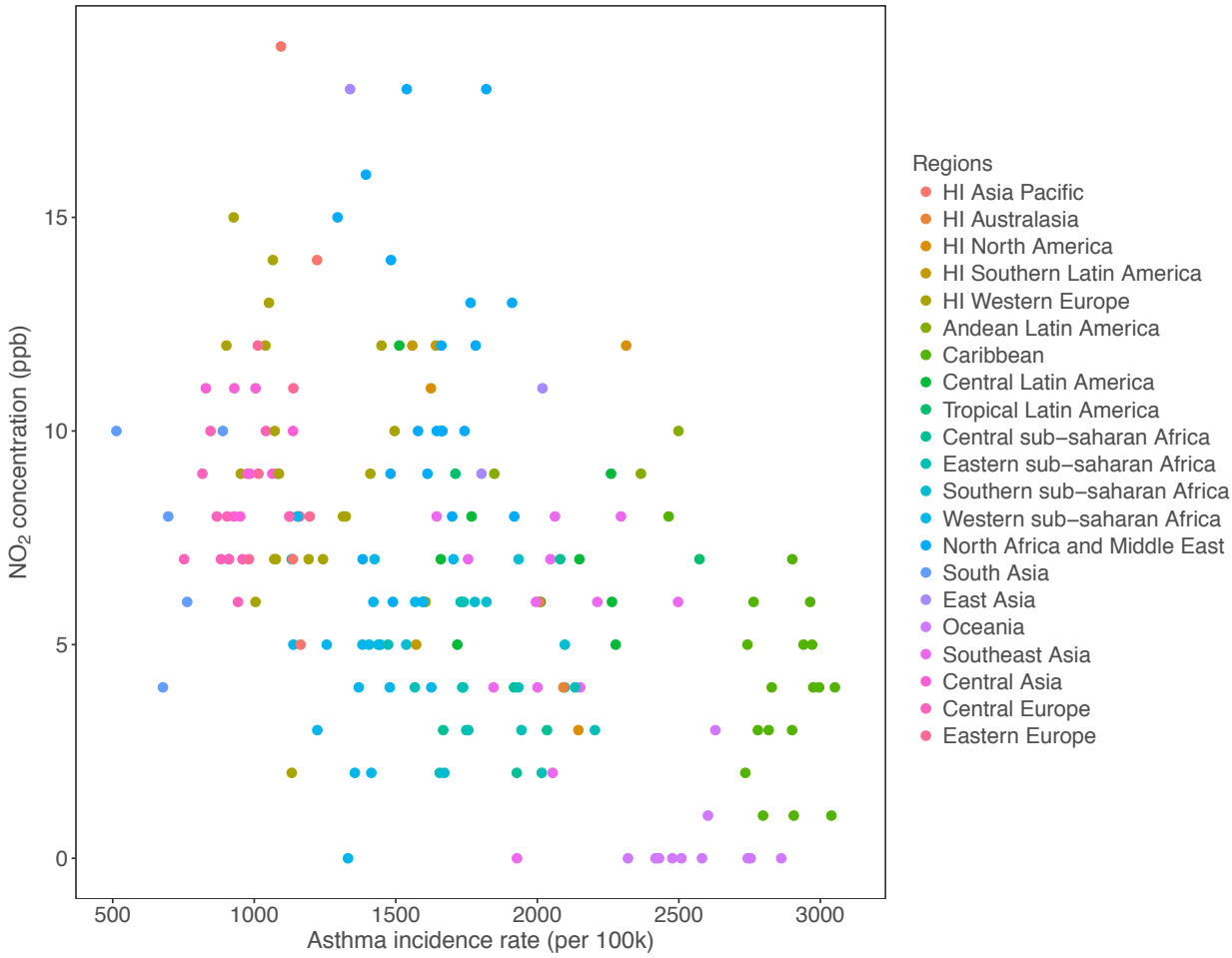

Figure S4. National estimates of population-weighted asthma incidence rates (per 100k children) versus population-weighted NO_2 concentrations (ppb). Colors represent different regions.

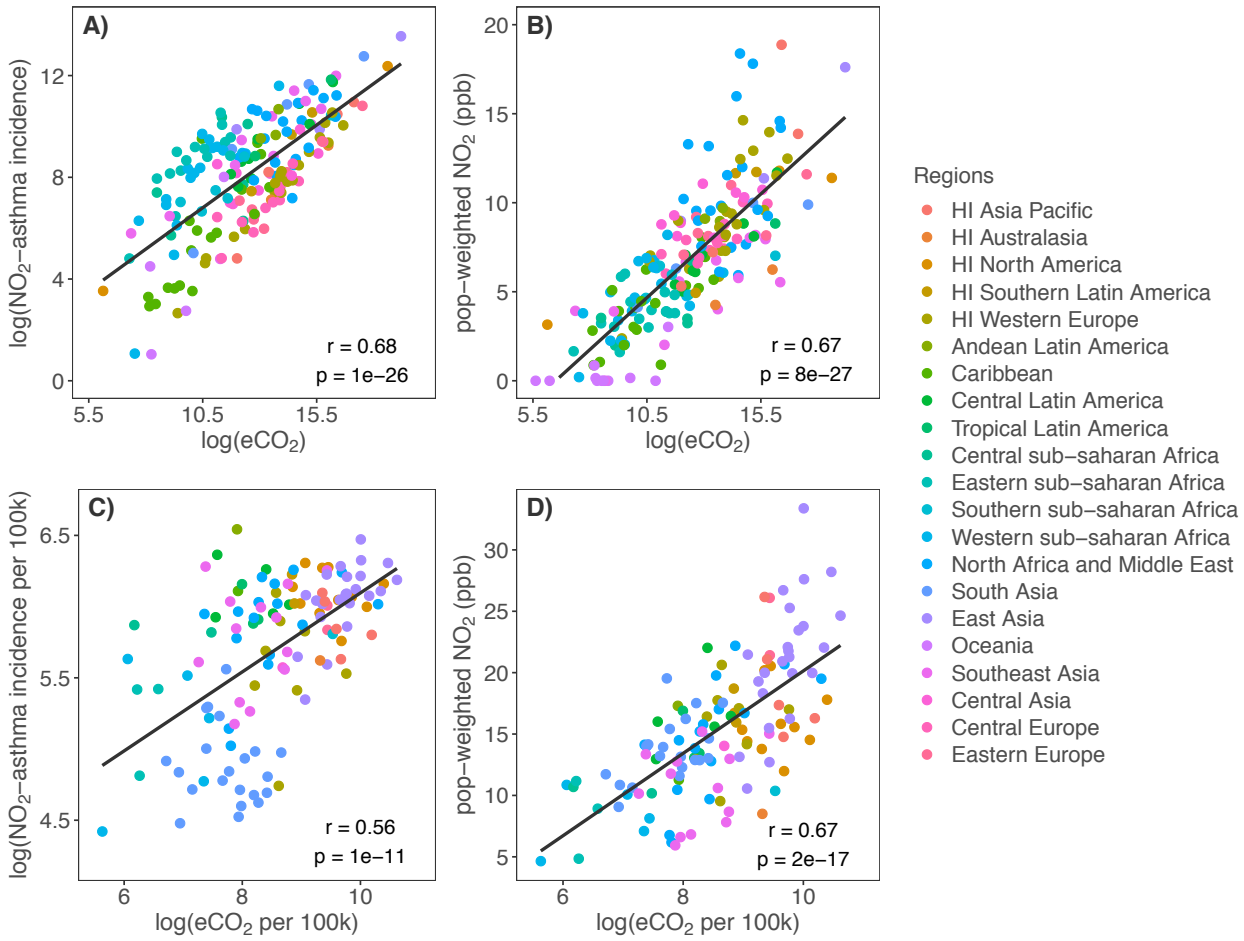

Figure S5. Top row: National estimates of A) annual NO_2-attributable asthma incidence (cases) and B) population-weighted annual average NO_2 concentrations (ppb) versus annual average CO_2 emissions (ton carbon) in 186 countries. Bottom row: Urban estimates of C) annual NO_2-attributable asthma incidence per 100k children and B) population-weighted annual average NO_2 concentrations versus annual average CO_2 emissions in 124 major cities. In B) and D), concentrations are weighted by the 1-18 year population size of each country/city. Note the log-scale on both x- and y-axes in all subplots except for population-weighted NO_2 concentrations. Country/city symbols are colored by region. The correlation coefficients, p-values, and linear regression lines are displayed inset.

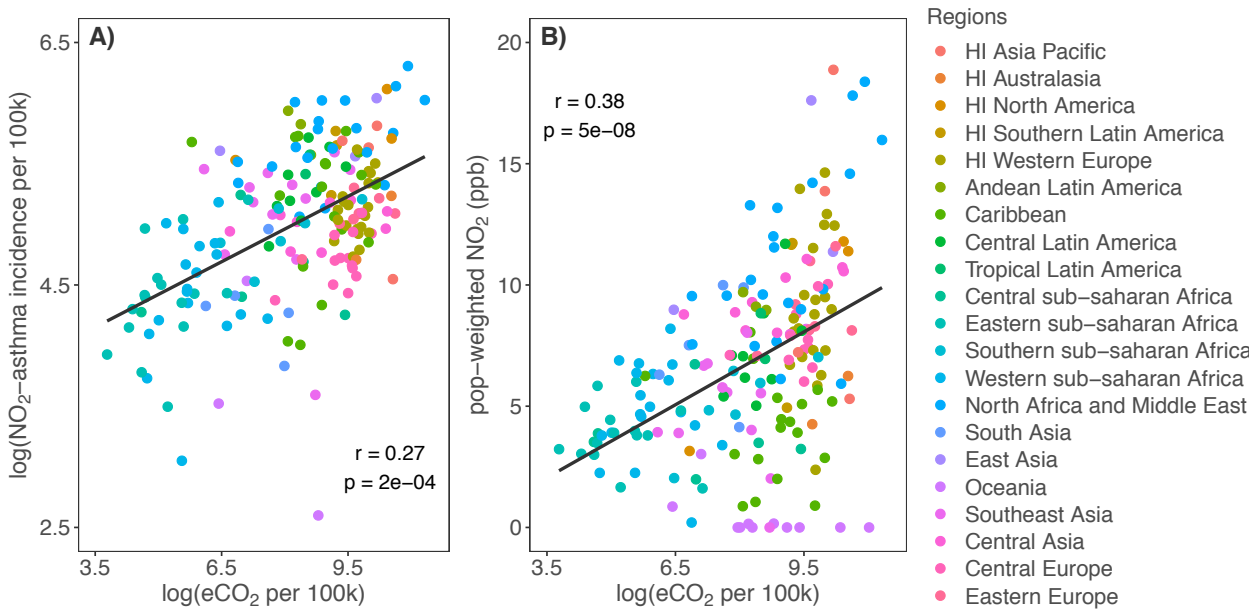

Figure S6. National estimates of A) annual NO_2-attributable asthma incidence per 100k children and B) paediatric population-weighted annual average NO_2 concentrations (ppb) versus annual average CO_2 emissions per 100k people in 186 countries. Country/city symbols are colored by region. The correlation coefficients, p-values, and linear regression lines are displayed inset.

Table S1. Description of meta-analyses of childhood asthma incidence attributable to traffic-related air pollution identified during our literature review. The relative risk estimates shown are for NO_2 as a pollutant (95% uncertainty intervals in parentheses).

Study	Relative risk per 10 ppb NO_2 (95% UI)	Relative risk per 10 µg m^{-3} $PM_{2.5}$ (95% UI)	Epidemiological model	Number of individual studies included	Cohort age	Cohort location
Khreis et al., 2017	1.26 (1.10-1.37)	1.34 (1.11-1.63)	Single-pollutant	20[a]	0-18 years	USA, Canada, Germany, Sweden, UK, Italy, The Netherlands, Japan, China, Korea
Bowatte et al., 2015	1.18 (0.93-1.48)	1.93 (1.00-3.71)	Single-pollutant	7	0-12 years	Sweden, Germany, Canada, Norway, the Netherlands
Anderson et al., 2013	1.24 (1.06-1.45)	*Not given*	Not specified	10	0-10 years	Europe, North America, Japan
Gasana et al., 2012	1.28 (1.12-1.50)	1.40 (0.77-2.56)	Some individual studies adjusted for co-pollutants	7	0-18 years	Europe, North America, Latin America, Asia

[a] 41 individual studies were reviewed but only 20 met their inclusion criteria for the NO_2 meta-analysis.

Table S2. Countries are grouped into 21 regions (which can be further grouped into 7 super-regions) following the Institute for Health Metrics and Evaluation (IHME) specification, which is based on two criteria: epidemiological similarity and geographic closeness.

Super-region	Regions	Countries
High-income	High-income Asia Pacific	Brunei, Japan, Singapore, South Korea
	High-income Australasia	Australia, New Zealand
	High-income North America	Canada, Greenland, United States
	High-income Southern Latin America	Argentina, Chile, Uruguay
	High-income Western Europe	Andorra, Austria, Belgium, Cyprus, Denmark, Finland, France, Germany, Greece, Iceland, Ireland, Israel, Italy, Luxembourg, Malta, Netherlands, Norway, Portugal, Spain, Sweden, Switzerland, United Kingdom
Latin America and Caribbean	Caribbean	Antigua and Barbuda, Barbados, Belize, Bermuda, Cuba, Dominica, Dominican Republic, Grenada, Guyana, Haiti, Jamaica, Puerto Rico, Saint Lucia, Saint Vincent and the Grenadines, Suriname, The Bahamas, Trinidad and Tobago, U.S. Virgin Islands
	Central Latin America	Colombia, Costa Rica, El Salvador, Guatemala, Honduras, Mexico, Nicaragua, Panama, Venezuela
	Tropical Latin America	Brazil, Paraguay
	Andean Latin America	Bolivia, Ecuador, Peru
Sub-Saharan Africa	Central sub-saharan Africa	Angola, Central African Republic, Congo, Democratic Republic of the Congo, Equatorial Guinea, Gabon
	Eastern sub-saharan Africa	Burundi, Comoros, Djibouti, Eritrea, Ethiopia, Kenya, Madagascar, Malawi, Mozambique, Rwanda, Somalia, South Sudan, Tanzania, Uganda, Zambia
	Southern sub-saharan Africa	Botswana, Lesotho, Namibia, South Africa, Swaziland, Zimbabwe
	Western sub-saharan Africa	Benin, Burkina Faso, Cameroon, Cape Verde, Chad, Côte d'Ivoire, Ghana, Guinea, Guinea-Bissau, Liberia, Mali, Mauritania, Niger, Nigeria, São Tomé and Príncipe, Senegal, Sierra Leone, The Gambia, Togo
North Africa and Middle East	North Africa and Middle East	Afghanistan, Algeria, Bahrain, Egypt, Iran, Iraq, Jordan, Kuwait, Lebanon, Libya, Morocco, Oman, Palestine, Qatar, Saudi Arabia, Sudan, Syria, Tunisia, Turkey, United Arab Emirates, Yemen
South Asia	South Asia	Bangladesh, Bhutan, India, Nepal, Pakistan
Southeast Asia, East Asia, and Oceania	East Asia	China, North Korea, Taiwan
	Oceania	American Samoa, Federated States of Micronesia, Fiji, Guam, Kiribati, Marshall Islands, Northern Mariana Islands, Papua New Guinea, Samoa, Solomon Islands, Tonga, Vanuatu
	Southeast Asia	Cambodia, Indonesia, Laos, Malaysia, Maldives, Mauritius, Myanmar, Philippines, Seychelles, Sri Lanka, Thailand, Timor-Leste, Vietnam
Central Europe, Eastern Europe, and Central Asia	Central Asia	Armenia, Azerbaijan, Georgia, Kazakhstan, Kyrgyzstan, Mongolia, Tajikistan, Turkmenistan, Uzbekistan
	Central Europe	Albania, Bosnia and Herzegovina, Bulgaria, Croatia, Czech Republic, Hungary, Macedonia, Montenegro, Poland, Romania, Serbia, Slovakia, Slovenia
	Eastern Europe	Belarus, Estonia, Latvia, Lithuania, Moldova, Russia, Ukraine

Table S3. Identification of the city or multiple cities (urban cluster) associated with a given GHS-SMOD raster id value for our target 125 major cities.

Primary city name	Urban cluster (if applicable)	GHS-SMOD id
Abidjan	Abidjan	1554
Accra	Tema-Accra	1756
Addis Ababa	Addis Ababa	4634
Ahmedabad	Ahmedabad	6178
Alexandria	Alexandria	3476
Algiers	Algiers	1926
Amman	Az Zarqa-Amman	4045
Ankara	Ankara	3522
Asyut	Mallawi-Asyut	3629
Baghdad	Baghdad	4790
Bandung	Bandung	12804
Bangalore	Bangalore	7703
Bangkok	Bangkok-Samut Sakhon-Pathum Thani-Nonthaburi-Samut Prakan	11083
Barcelona	Barcelona-Mataro	1895
Beijing	Beijing-Changping	11054
Belo Horizonte	Belo Horizonte	1244
Bogota	Bogota	575
Buenos Aires	Buenos Aires	1014
Busan	Busan	13406
Cairo	Cairo-El Giza-Benha-Zagazig-El Mansura-Tanta	3560
Caracas	Caracas-Los Teques	781
Casablanca	Casablanca	1464
Chengdu	Chengdu	10585
Chennai	Chennai	8434
Chicago	Chicago-Joliet-Evanston-Elgin-Waukegan-Aurora-Gary	587
Chittagong	Chittagong	10266
Chongqing	Chongqing	10935
Cologne	Dortmund-Duisburg-Wuppertal-Essen-Bonn-Ddsseldorf-Cologne	2114
Colombo	Moratuwa-Sri Jawewardenepura Kotte-Colombo	8619
Dallas	Arlington-Ft. Worth-Dallas	310
Dar es Salaam	Dar es Salaam	4720
DC	Washington, D.C.-Alexandria	780
Dhaka	Narayanganj-Dhaka	9953
Dubai	Dubai-Sharjah	5297
Faisalabad	Faisalabad	5877
Fuzhou	Fuzhou	13301

Guadalajara	Guadalajara	93
Guangzhou	Jiangmen-Foshan-Guangzhou-Shenzhen-Huizhou-Dongguan	12827
Hangzhou	Hangzhou-Shaoxing	13124
Hanoi	Bac Giang-Son Tay-Hanoi	11559
Harbin	Harbin	11563
HCMC	Thu Dau Mot-Bien Hoa-Ho Chi Minh City	12519
Hefei	Hefei	12628
Houston	Pasadena-Houston	300
Hyderabad	Hyderabad	7648
Istanbul	Istanbul	3298
Jaipur	Jaipur	6465
Jakarta	Jakarta-Serang-Bekasi-Bogor	12584
Jeddah	Jeddah	4492
Johannesburg	Johannesburg-Springs-Benoni-Pretoria	3403
Kabul	Kabul	5543
Kano	Kano	2516
Kanpur	Kanpur	7395
Karachi	Karachi	5587
Kathmandu	Lalitpur-Kathmandu	8521
Khartoum	Omdurman-Khartoum	3962
Kinshasa	Kinshasa-Brazzaville	2970
Kolkata	Haora-Kolkata	9612
Kuala Lumpur	Kuala Lumpur-Shah Alam-Kelang-Putrajaya	11607
Lagos	Lagos	1960
Lahore	Lahore-Sheikhu Pura	5956
Lima	Lima	494
London	London	1761
Los Angeles	Los Angeles-Riverside-Pasadena-Irvine-Long Beach-San Bernardino	15
Luanda	Luanda	2834
Lucknow	Lucknow	7490
Madrid	Madrid	1577
Manchester	Manchester-Liverpool	1621
Manila	Manila-Quezon City-Pasay City	13542
Medan	Binjai-Medan	11065
Mexico City	Mexico City-Nezahualcoyotl	157
Miami	Miami-Homestead-Coral Springs-Coral Gables-Fort Lauderdale	513
Milan	Milan-Como	2350
Monterrey	Monterrey	202
Moscow	Moscow-Podolsk	3409

Mumbai	Mumbai-Kalyan	6400
Nagoya	Gifu-Tsu-Nagoya	13644
Nairobi	Nairobi	4414
Nanjing	Nanjing	12812
Naples	Caserta-Naples	2775
New Delhi	New Delhi-Gurgaon-Sonipat-Ghaziabad-Faridabad-Delhi	6542
NYC	Paterson-Newark-New York	864
Orlu	Orlu-Onitsha	2304
Osaka	Osaka-Otsu-Kobe-Kyoto	13577
Paris	Paris-Versailles-Melun	1892
Peshawar	Mardan-Peshawar	5625
Philadelphia	Wilmington-Trenton-Philadelphia	826
Pune	Pune	6628
Qingdao	Qingdao	12481
Quanzhou	Quanzhou	13313
Rangoon	Rangoon	10518
Rawalpindi	Rawalpindi	5772
Rio de Janeiro	Rio de Janeiro-Nova Iguacu-Duque de Caxias	1262
Riyadh	Riyadh	5119
San Diego	Tijuana-National City-San Diego	23
San Francisco	San Francisco-Berkeley-San Mateo-Oakland-San Jose	11
Santiago	Santiago-San Bernardo	852
Santo Domingo	San Cristobal-Santo Domingo	748
Sao Paulo	Sao Paulo-Santo Andre	1204
Semarang	Pati-Semarang	13121
Seoul	Seoul-Ansan-Puch'on-Songnam-Goyang-Suwon-Incheon	13127
Shanghai	Shanghai	13141
Shantou	Chaozhou-Shantou	13174
Shenyang	Shenyeng	11918
Singapore	Singapore-Johor Bahru	12102
Sohag	Sohag-Girga	3690
St Petersburg	St. Petersburg	3147
Surabaya	Mojokerto-Surabaya	13307
Surakarta	Yogyakarta-Surakarta	13131
Surat	Surat	6280
Sydney	Sydney	13793
Taipei	Taipei-Bade-Pingzhen-Taoyuan-Yangmei-Zhongli-Keelung-New Taipei	13423
Taiyuan	Taiyuan	10873
Tashkent	Tashkent	5387

Tehran	Tehran-Karaj	5137
Tianjin	Tianjin	11319
Tokyo	Tokyo-Kawasaki-Kawagoe-Hachioji-Yokohama	13701
Toronto	Toronto	801
Varanasi	Varanasi	8185
Wenzhou	Wenzhou	13318
Wuhan	Wuhan	12200
Wuxi	Changzhou-Wuxi-Suzhou	12992
Xi'an	Xianyang-Xian	10776
Xiamen	Xiamen	13266
Zhengzhou	Zhengzhou	11443

Table S4. Population and disability-adjusted life years (DALYs, or years of healthy life lost) due to asthma for children aged 1-18 years. Countries are grouped into regions according to the IHME specification (Table S2). Numbers are rounded to 2 significant figures.

Regions	**1-18y population (millions)**	**Number of DALYs due to asthma from NO_2 exposure (thousands per year)**
High-income Asia Pacific	33	19
High-income Australasia	6.7	3.0
High-income North America	86	43
High-income Southern Latin America	19	12
High-income Western Europe	83	44
Andean Latin America	22	13
Caribbean	14	9.3
Central Latin America	92	39
Tropical Latin America	64	26
Central sub-saharan Africa	57	13
Eastern sub-saharan Africa	190	32
Southern sub-saharan Africa	29	10
Western sub-saharan Africa	190	41
North Africa and Middle East	210	110
South Asia	640	110
East Asia	310	100
Oceania	3.8	0.69
Southeast Asia	220	70
Central Asia	30	8.6
Central Europe	22	5.9
Eastern Europe	39	14
GLOBAL	2,400	730

Table S5. National sums of population, total paediatric asthma incidence, and NO_2-attributable incidence assuming counterfactual concentrations of 0ppb, 2ppb, and 5ppb. The estimates shown are derived using the central mean relative risk (RR) value from Khreis et al. (2017), with the 95% uncertainty intervals reflecting uncertainty in the RR shown in parentheses for the number of cases. Results are rounded to 2 significant figures.

		Number of new asthma cases (thousands per year)			
Country	**1-18y population**	**Total**	**0ppb**	**2ppb**	**5ppb**
Afghanistan	1.70E+07	290	56 (25-74)	43 (19-56)	25 (11-32)
Albania	7.90E+05	5.9	0.89 (0.39-1.2)	0.62 (0.28-0.81)	0.26 (0.12-0.33)
Algeria	1.40E+07	230	38 (17-51)	28 (12-36)	13 (6.1-17)
American Samoa	2.30E+04	0.58	0 (0-0)	0 (0-0)	0 (0-0)
Andorra	1.20E+04	0.13	0.02 (0.0088-0.027)	0.014 (0.0063-0.019)	0.0058 (0.0026-0.0075)
Angola	1.30E+07	270	36 (16-48)	24 (11-32)	9.9 (4.5-13)
Antigua and Barbuda	2.70E+04	0.75	0.07 (0.03-0.094)	0.038 (0.016-0.05)	0.007 (0.0031-0.009)
Argentina	1.30E+07	210	48 (21-62)	38 (17-49)	25 (12-31)
Armenia	7.30E+05	7.2	1.4 (0.63-1.9)	1.1 (0.49-1.4)	0.65 (0.3-0.82)
Australia	5.60E+06	110	15 (6.7-20)	10 (4.6-14)	4.5 (2.1-5.8)
Austria	1.60E+06	17	3.3 (1.4-4.3)	2.5 (1.1-3.3)	1.4 (0.67-1.8)
Azerbaijan	2.90E+06	27	4.7 (2.1-6.2)	3.5 (1.5-4.5)	1.7 (0.8-2.2)
Bahrain	6.40E+05	10	3.1 (1.4-4)	2.6 (1.2-3.4)	2 (0.94-2.5)
Bangladesh	6.40E+07	440	72 (32-95)	52 (23-68)	25 (11-31)
Barbados	6.80E+04	2	0.26 (0.11-0.35)	0.17 (0.074-0.22)	0.052 (0.023-0.067)
Belarus	1.80E+06	21	4.6 (2-5.9)	3.6 (1.7-4.7)	2.3 (1.1-2.9)
Belgium	2.30E+06	21	5.8 (2.6-7.4)	4.8 (2.2-6.1)	3.4 (1.6-4.3)
Belize	1.50E+05	4.5	0.57 (0.25-0.76)	0.37 (0.16-0.48)	0.11 (0.05-0.14)
Benin	5.60E+06	77	7.8 (3.3-10)	4.3 (1.9-5.7)	0.84 (0.38-1.1)
Bermuda	1.20E+04	0.36	0.055 (0.024-0.073)	0.039 (0.017-0.051)	0.016 (0.0074-0.021)
Bhutan	3.30E+05	2.2	0.25 (0.11-0.34)	0.15 (0.066-0.2)	0.046 (0.021-0.059)
Bolivia	4.10E+06	96	18 (8-24)	14 (6.2-18)	7.9 (3.7-10)
Bosnia and Herzegovina	7.60E+05	6.7	0.99 (0.43-1.3)	0.68 (0.3-0.9)	0.26 (0.12-0.34)
Botswana	8.70E+05	15	2 (0.86-2.7)	1.3 (0.57-1.7)	0.33 (0.15-0.42)
Brazil	6.20E+07	1100	190 (82-240)	140 (63-180)	77 (36-97)
Brunei	1.30E+05	1.5	0.19 (0.082-0.25)	0.12 (0.054-0.16)	0.047 (0.021-0.06)
Bulgaria	1.20E+06	11	1.7 (0.74-2.2)	1.2 (0.54-1.6)	0.54 (0.25-0.7)
Burkina Faso	9.20E+06	150	20 (8.5-26)	13 (5.8-17)	4.2 (1.9-5.4)
Burundi	5.60E+06	98	7.1 (3-9.5)	2.8 (1.2-3.8)	0.24 (0.11-0.31)
Cambodia	6.40E+06	130	19 (8.2-25)	13 (5.7-17)	5.1 (2.3-6.5)
Cameroon	1.10E+07	140	16 (7-22)	9.9 (4.3-13)	3.1 (1.4-4)
Canada	7.50E+06	170	42 (19-54)	34 (15-43)	23 (11-29)
Cape Verde	2.10E+05	2.5	0.25 (0.11-0.33)	0.14 (0.061-0.19)	0.02 (0.0088-0.026)
Central African Republic	2.30E+06	44	3.4 (1.5-4.5)	1.6 (0.72-2.2)	0.46 (0.21-0.59)
Chad	7.60E+06	110	14 (6.2-19)	9.4 (4.1-12)	2.8 (1.2-3.6)

Chile	5.00E+06	82	20 (9-25)	16 (7.4-20)	11 (5.2-14)
China	2.90E+08	3900	940 (430-1200)	760 (350-970)	510 (240-640)
Colombia	1.80E+07	400	72 (32-94)	54 (24-69)	31 (15-39)
Comoros	3.70E+05	7.5	0.33 (0.14-0.45)	0.12 (0.053-0.16)	0.0024 (0.0011-0.0031)
Congo	2.10E+06	34	3.6 (1.6-4.8)	2.2 (0.99-2.9)	0.94 (0.43-1.2)
Costa Rica	1.50E+06	34	4.4 (1.9-5.8)	2.9 (1.3-3.8)	1.1 (0.48-1.4)
Cote d'Ivoire	1.10E+07	160	14 (6.2-19)	7.6 (3.3-9.9)	2.4 (1.1-3)
Croatia	8.00E+05	7.6	1.2 (0.54-1.6)	0.89 (0.4-1.2)	0.42 (0.19-0.54)
Cuba	2.40E+06	70	11 (4.6-14)	7.4 (3.3-9.7)	3.1 (1.4-4)
Cyprus	2.40E+05	2.5	0.5 (0.22-0.65)	0.39 (0.17-0.5)	0.23 (0.11-0.3)
Czech Republic	1.90E+06	16	3.3 (1.4-4.3)	2.6 (1.2-3.3)	1.6 (0.72-2)
Democratic Republic of the Congo	3.90E+07	820	62 (26-82)	32 (14-41)	11 (5-14)
Denmark	1.20E+06	13	2.4 (1-3.1)	1.8 (0.79-2.3)	0.92 (0.42-1.2)
Djibouti	3.50E+05	5.9	0.91 (0.39-1.2)	0.64 (0.28-0.84)	0.27 (0.12-0.35)
Dominica	2.60E+04	0.72	0.053 (0.023-0.071)	0.027 (0.012-0.036)	0.0055 (0.0025-0.0072)
Dominican Republic	3.80E+06	94	16 (7-21)	12 (5.2-15)	6 (2.8-7.7)
Ecuador	6.00E+06	110	21 (9.2-27)	16 (7.1-20)	9.1 (4.2-11)
Egypt	3.60E+07	620	120 (54-150)	91 (42-120)	53 (26-66)
El Salvador	2.50E+06	53	7.9 (3.5-10)	5.5 (2.4-7.2)	2.3 (1.1-3)
Equatorial Guinea	3.70E+05	7.2	0.6 (0.25-0.8)	0.3 (0.13-0.4)	0.066 (0.03-0.086)
Eritrea	2.50E+06	43	5.8 (2.5-7.8)	3.9 (1.7-5.1)	1.1 (0.51-1.5)
Estonia	2.40E+05	2.8	0.52 (0.23-0.68)	0.4 (0.18-0.51)	0.22 (0.1-0.28)
Ethiopia	5.10E+07	740	71 (30-94)	38 (16-50)	5.8 (2.6-7.4)
Federated States of Micronesia	4.40E+04	1.1	0.0058 (0.0025-0.0078)	0.0028 (0.0012-0.0037)	0.00051 (0.00023-0.00066)
Finland	1.10E+06	17	3.3 (1.5-4.3)	2.5 (1.1-3.3)	1.5 (0.69-1.9)
France	1.40E+07	150	32 (15-42)	26 (12-33)	16 (7.6-20)
Gabon	7.60E+05	16	1.2 (0.49-1.6)	0.54 (0.23-0.71)	0.089 (0.04-0.12)
Georgia	8.80E+05	8.4	1.4 (0.62-1.9)	1 (0.46-1.4)	0.53 (0.24-0.67)
Germany	1.30E+07	120	28 (13-37)	23 (10-30)	15 (7.1-19)
Ghana	1.20E+07	140	14 (5.9-18)	7.7 (3.4-10)	2.2 (0.97-2.8)
Greece	1.90E+06	18	3.5 (1.5-4.5)	2.6 (1.2-3.4)	1.5 (0.72-2)
Greenland	1.40E+04	0.29	0.047 (0.02-0.062)	0.034 (0.015-0.045)	0.017 (0.0075-0.021)
Grenada	3.70E+04	1.1	0.052 (0.022-0.069)	0.02 (0.0089-0.027)	0.0028 (0.0012-0.0036)
Guam	5.50E+04	1.3	0 (0-0)	0 (0-0)	0 (0-0)
Guatemala	7.70E+06	130	19 (8.4-25)	13 (5.9-17)	5.7 (2.6-7.3)
Guinea	6.20E+06	100	8.7 (3.7-12)	4.2 (1.8-5.5)	0.51 (0.23-0.67)
Guinea-Bissau	9.00E+05	12	1.1 (0.45-1.4)	0.54 (0.23-0.72)	0.055 (0.025-0.072)
Guyana	2.90E+05	8	0.89 (0.38-1.2)	0.54 (0.24-0.71)	0.16 (0.073-0.21)
Haiti	4.70E+06	140	20 (8.6-26)	14 (6.1-18)	6.4 (2.9-8.2)
Honduras	3.40E+06	69	9.3 (4-12)	6.2 (2.7-8.1)	2.5 (1.2-3.2)

Hungary	1.80E+06	15	2.7 (1.2-3.5)	2 (0.91-2.6)	1.1 (0.5-1.4)
Iceland	8.40E+04	1	0.17 (0.074-0.22)	0.12 (0.055-0.16)	0.058 (0.026-0.074)
India	4.90E+08	2500	460 (200-600)	350 (160-450)	190 (87-240)
Indonesia	8.80E+07	1900	250 (110-330)	160 (72-210)	67 (31-85)
Iran	2.30E+07	340	90 (41-120)	75 (35-95)	53 (25-66)
Iraq	1.70E+07	280	68 (30-88)	55 (25-71)	37 (17-47)
Ireland	1.20E+06	19	2.5 (1.1-3.3)	1.7 (0.74-2.2)	0.64 (0.29-0.83)
Israel	2.60E+06	27	6.5 (2.9-8.5)	5.3 (2.4-6.9)	3.7 (1.7-4.6)
Italy	1.00E+07	80	15 (6.8-20)	12 (5.2-15)	6.7 (3.1-8.5)
Jamaica	9.10E+05	25	2.9 (1.3-3.9)	1.8 (0.81-2.4)	0.71 (0.32-0.9)
Japan	2.10E+07	250	69 (32-88)	57 (27-73)	41 (20-52)
Jordan	3.30E+06	63	17 (7.5-21)	14 (6.3-17)	9.6 (4.5-12)
Kazakhstan	5.30E+06	44	9.6 (4.3-13)	7.6 (3.4-9.8)	4.8 (2.2-6.1)
Kenya	2.20E+07	350	29 (12-39)	14 (6.2-19)	3.4 (1.5-4.4)
Kiribati	4.10E+03	0.11	0 (0-0)	0 (0-0)	0 (0-0)
Kuwait	1.10E+06	20	7 (3.3-8.9)	6.1 (2.9-7.7)	4.8 (2.3-5.9)
Kyrgyzstan	2.20E+06	23	4.6 (2-6)	3.5 (1.6-4.6)	2 (0.93-2.6)
Laos	3.00E+06	60	7.5 (3.2-9.9)	4.8 (2.1-6.3)	1.6 (0.7-2)
Latvia	3.50E+05	4.1	0.75 (0.33-0.99)	0.57 (0.25-0.74)	0.31 (0.14-0.4)
Lebanon	1.80E+06	32	8.7 (4-11)	7.3 (3.4-9.2)	5.3 (2.5-6.5)
Lesotho	8.90E+05	15	1.8 (0.77-2.4)	1.1 (0.49-1.5)	0.2 (0.09-0.26)
Liberia	2.10E+06	29	1.5 (0.63-2)	0.45 (0.19-0.6)	0.036 (0.016-0.046)
Libya	2.40E+06	38	6.5 (2.9-8.6)	4.8 (2.1-6.3)	2.4 (1.1-3.1)
Lithuania	5.60E+05	5.7	1.1 (0.48-1.4)	0.84 (0.37-1.1)	0.47 (0.22-0.61)
Luxembourg	1.20E+05	1.7	0.36 (0.16-0.47)	0.29 (0.13-0.37)	0.18 (0.084-0.23)
Macedonia	4.70E+05	4.2	0.7 (0.31-0.93)	0.51 (0.23-0.67)	0.24 (0.11-0.31)
Madagascar	1.20E+07	230	18 (7.8-24)	9.8 (4.3-13)	1.6 (0.74-2.1)
Malawi	8.60E+06	150	13 (5.7-18)	6.7 (2.9-8.9)	0.42 (0.19-0.55)
Malaysia	1.00E+07	210	33 (15-44)	24 (11-31)	13 (6.1-16)
Maldives	1.40E+05	2.6	0.42 (0.18-0.54)	0.33 (0.15-0.43)	0.2 (0.094-0.26)
Mali	9.20E+06	100	15 (6.3-19)	9.8 (4.3-13)	3.4 (1.5-4.3)
Malta	7.90E+04	0.94	0.14 (0.063-0.19)	0.1 (0.045-0.13)	0.044 (0.02-0.056)
Marshall Islands	8.00E+03	0.2	0 (0-0)	0 (0-0)	0 (0-0)
Mauritania	2.00E+06	34	5.1 (2.2-6.7)	3.5 (1.6-4.6)	1.4 (0.62-1.8)
Mauritius	3.30E+05	6.8	0.31 (0.13-0.42)	0.12 (0.052-0.16)	0.017 (0.0075-0.022)
Mexico	4.50E+07	680	160 (71-200)	130 (58-160)	84 (40-110)
Moldova	1.10E+06	11	1.7 (0.72-2.2)	1.2 (0.52-1.6)	0.52 (0.23-0.67)
Mongolia	9.80E+05	9.9	2.2 (0.99-2.9)	1.8 (0.8-2.3)	1.1 (0.53-1.5)
Montenegro	1.50E+05	1.4	0.19 (0.08-0.25)	0.12 (0.054-0.16)	0.042 (0.019-0.054)
Morocco	1.10E+07	160	25 (11-33)	18 (8-23)	8.2 (3.8-11)
Mozambique	1.40E+07	270	24 (10-32)	12 (5.2-16)	1.7 (0.76-2.2)

Myanmar	1.80E+07	320	47 (21-63)	33 (14-43)	13 (5.8-17)
Namibia	1.10E+06	19	2.7 (1.1-3.5)	1.8 (0.78-2.3)	0.57 (0.26-0.74)
Nepal	1.20E+07	91	13 (5.7-17)	9 (4-12)	3.4 (1.6-4.4)
Netherlands	3.60E+06	38	9.8 (4.4-13)	8.1 (3.7-10)	5.7 (2.7-7.2)
New Zealand	1.10E+06	23	2.2 (0.93-2.9)	1.2 (0.54-1.6)	0.35 (0.16-0.45)
Nicaragua	2.70E+06	47	5.5 (2.4-7.3)	3.4 (1.5-4.4)	0.89 (0.4-1.1)
Niger	1.10E+07	160	24 (10-31)	16 (7.2-22)	6.4 (2.9-8.3)
Nigeria	8.60E+07	1400	170 (73-230)	110 (48-140)	33 (15-43)
Northern Mariana Islands	1.50E+04	0.41	0 (0-0)	0 (0-0)	0 (0-0)
North Korea	7.20E+06	130	26 (11-33)	20 (8.8-26)	11 (5.2-15)
Norway	1.20E+06	13	2.2 (0.97-2.9)	1.6 (0.73-2.1)	0.86 (0.4-1.1)
Oman	1.20E+06	19	4 (1.8-5.3)	3.2 (1.4-4.1)	1.9 (0.87-2.4)
Pakistan	8.10E+07	720	150 (66-190)	120 (52-150)	69 (32-88)
Palestine	2.30E+06	39	8.3 (3.7-11)	6.5 (2.9-8.4)	4.1 (1.9-5.2)
Panama	1.30E+06	31	3.4 (1.5-4.6)	2.1 (0.9-2.7)	0.57 (0.26-0.73)
Papua New Guinea	3.20E+06	85	6.2 (2.7-8.3)	3 (1.3-4)	0.57 (0.26-0.73)
Paraguay	2.60E+06	67	9.9 (4.3-13)	6.9 (3-9)	2.9 (1.3-3.7)
Peru	1.10E+07	290	56 (25-73)	43 (20-56)	27 (12-33)
Philippines	4.00E+07	990	130 (58-170)	90 (41-120)	46 (22-58)
Poland	7.40E+06	77	15 (6.8-20)	12 (5.4-16)	7.1 (3.3-9.1)
Portugal	1.90E+06	25	4.2 (1.9-5.6)	3.2 (1.4-4.1)	1.7 (0.79-2.2)
Puerto Rico	9.10E+05	25	3.1 (1.4-4.1)	2 (0.89-2.6)	0.87 (0.4-1.1)
Qatar	3.20E+05	4.4	1.5 (0.71-1.9)	1.3 (0.62-1.6)	1 (0.5-1.3)
Romania	3.80E+06	42	7 (3.1-9.2)	5.1 (2.3-6.7)	2.4 (1.1-3.1)
Russia	2.70E+07	270	62 (28-80)	50 (23-63)	32 (15-40)
Rwanda	5.50E+06	120	8.8 (3.7-12)	3.5 (1.5-4.6)	0.32 (0.15-0.42)
Saint Lucia	5.50E+04	1.5	0.096 (0.041-0.13)	0.042 (0.018-0.056)	0.0087 (0.0039-0.011)
Saint Vincent and the Grenadines	3.30E+04	0.93	0.052 (0.022-0.069)	0.019 (0.0081-0.025)	0.0022 (0.00099-0.0029)
Samoa	4.00E+03	0.092	0 (0-0)	0 (0-0)	0 (0-0)
Sao Tome and Principe	8.80E+04	1.2	0.0062 (0.0026-0.0084)	0.0029 (0.0013-0.0039)	1.4e-05 (6.1e-06-1.8e-05)
Saudi Arabia	1.00E+07	130	38 (18-49)	32 (15-41)	24 (11-30)
Senegal	7.40E+06	85	12 (5.4-16)	8.6 (3.8-11)	3.3 (1.5-4.3)
Serbia	1.20E+06	14	2.4 (1-3.1)	1.7 (0.77-2.3)	0.86 (0.39-1.1)
Seychelles	2.60E+04	0.51	4.2e-07 (1.8e-07-5.6e-07)	2.1e-07 (8.8e-08-2.7e-07)	0 (0-0)
Sierra Leone	3.00E+06	43	3 (1.3-4)	1.3 (0.55-1.7)	0.29 (0.13-0.38)
Singapore	1.20E+06	14	4.3 (2-5.5)	3.7 (1.7-4.6)	2.8 (1.3-3.5)
Slovakia	1.10E+06	9.2	1.5 (0.67-2)	1.1 (0.49-1.5)	0.53 (0.24-0.68)
Slovenia	3.50E+05	3.2	0.49 (0.21-0.65)	0.34 (0.15-0.45)	0.14 (0.066-0.19)
Solomon Islands	2.70E+05	6.9	0.2 (0.084-0.26)	0.09 (0.039-0.12)	0.015 (0.0068-0.02)
Somalia	5.70E+06	98	13 (5.4-17)	8.1 (3.5-11)	2.4 (1.1-3.1)

South Africa	1.90E+07	360	50 (22-67)	34 (15-45)	14 (6.3-18)
South Korea	1.10E+07	120	41 (19-51)	36 (17-44)	28 (14-34)
South Sudan	6.10E+06	110	11 (4.5-14)	5.8 (2.5-7.7)	0.68 (0.3-0.88)
Spain	8.20E+06	88	18 (8.1-24)	14 (6.5-18)	8.8 (4.1-11)
Sri Lanka	6.20E+06	120	12 (5.3-17)	6.9 (3-9)	1.8 (0.82-2.3)
Sudan	2.00E+07	380	58 (25-76)	41 (18-53)	17 (7.7-22)
Suriname	1.80E+05	5.4	0.52 (0.22-0.69)	0.28 (0.12-0.37)	0.078 (0.035-0.1)
Swaziland	6.00E+05	13	1.4 (0.58-1.8)	0.78 (0.34-1)	0.1 (0.046-0.13)
Sweden	2.00E+06	27	5 (2.2-6.5)	3.8 (1.7-4.9)	2.1 (0.96-2.7)
Switzerland	1.50E+06	17	3.1 (1.4-4.1)	2.4 (1.1-3.1)	1.3 (0.6-1.7)
Syria	7.70E+06	140	33 (15-43)	27 (12-34)	18 (8.4-23)
Taiwan	4.70E+06	95	24 (11-31)	20 (9.2-25)	14 (6.5-17)
Tajikistan	3.60E+06	35	6.6 (2.9-8.6)	5 (2.2-6.5)	2.8 (1.3-3.6)
Tanzania	2.60E+07	560	47 (20-63)	24 (10-31)	2.5 (1.1-3.3)
Thailand	1.60E+07	380	61 (27-80)	44 (20-57)	21 (9.9-27)
The Bahamas	1.30E+05	3.6	0.5 (0.22-0.66)	0.34 (0.15-0.44)	0.13 (0.061-0.17)
The Gambia	1.00E+06	14	1.6 (0.71-2.2)	1 (0.44-1.3)	0.23 (0.1-0.3)
Timor-Leste	5.60E+05	12	1.1 (0.49-1.5)	0.65 (0.29-0.85)	0.23 (0.1-0.29)
Togo	3.40E+06	50	5.2 (2.2-6.9)	2.9 (1.3-3.9)	0.54 (0.24-0.69)
Tonga	4.40E+04	1.3	0 (0-0)	0 (0-0)	0 (0-0)
Trinidad and Tobago	3.40E+05	10	1.1 (0.49-1.5)	0.7 (0.31-0.92)	0.23 (0.1-0.29)
Tunisia	3.20E+06	47	7.5 (3.3-9.8)	5.3 (2.4-7)	2.5 (1.1-3.1)
Turkey	2.40E+07	360	83 (38-110)	67 (31-86)	44 (21-56)
Turkmenistan	1.90E+06	18	4 (1.8-5.2)	3.2 (1.4-4.1)	2 (0.95-2.6)
Uganda	2.10E+07	370	24 (10-32)	9.2 (4-12)	1.2 (0.56-1.6)
Ukraine	7.90E+06	95	17 (7.3-22)	12 (5.5-16)	6.3 (2.9-8)
United Arab Emirates	2.10E+06	32	11 (5.1-14)	9.5 (4.5-12)	7.5 (3.6-9.3)
United Kingdom	1.40E+07	200	47 (21-61)	38 (17-49)	25 (12-32)
United States	7.80E+07	1300	290 (130-380)	240 (110-300)	160 (73-190)
Uruguay	9.20E+05	14	2.4 (1-3.1)	1.7 (0.77-2.2)	0.83 (0.38-1.1)
Uzbekistan	1.10E+07	130	25 (11-33)	20 (8.8-25)	12 (5.3-15)
Vanuatu	1.20E+05	3	0.039 (0.016-0.052)	0.016 (0.0067-0.021)	0.00074 (0.00033-0.00095)
Venezuela	1.00E+07	180	32 (14-42)	24 (11-31)	13 (6.1-17)
Vietnam	2.90E+07	480	81 (36-110)	60 (27-77)	30 (14-38)
Virgin Islands, U.S.	2.70E+04	0.77	0.067 (0.029-0.089)	0.034 (0.015-0.045)	0.0062 (0.0028-0.0081)
Yemen	1.40E+07	220	43 (19-57)	33 (15-43)	19 (8.9-25)
Zambia	8.30E+06	120	12 (5.3-17)	7 (3-9.2)	1.2 (0.55-1.6)
Zimbabwe	7.30E+06	110	12 (5-16)	6.8 (2.9-8.9)	0.81 (0.36-1)
GLOBAL	2.40E+09	32000	5400 (2400-7100)	4000 (1800-5200)	2300 (1100-2900)

Table S6. National sums of (A) NO_2-attributable paediatric asthma incidence per 100k children, (B) percentage of total incidence attributable to NO_2, and (C) percentage of NO_2-attributable incidence that occurred in urban centers, assuming a counterfactual concentration of 2ppb. The estimates shown are derived using the central mean relative risk (RR) value from Khreis et al. (2017), with the 95% uncertainty intervals for (A)-(B) reflecting uncertainty in the RR shown in parentheses. Results are rounded to 2 significant figures.

Country	Cases per year per 100k	NO2-attributable percentage	Urban percentage
Afghanistan	250 (110-320)	15 (6.8-20)	48
Albania	79 (35-100)	11 (4.7-14)	55
Algeria	200 (90-260)	12 (5.3-15)	55
American Samoa	0 (0-0)	0 (0-0)	0
Andorra	120 (53-160)	11 (4.7-14)	0
Angola	190 (84-250)	9.1 (4-12)	81
Antigua and Barbuda	140 (62-190)	5 (2.2-6.6)	0
Argentina	280 (130-360)	18 (8.3-23)	76
Armenia	150 (68-200)	15 (6.9-20)	50
Australia	190 (83-250)	9.4 (4.1-12)	77
Austria	160 (73-210)	15 (6.7-19)	45
Azerbaijan	120 (52-150)	13 (5.6-16)	48
Bahrain	410 (190-520)	26 (12-32)	98
Bangladesh	82 (37-110)	12 (5.3-15)	76
Barbados	250 (110-320)	8.2 (3.6-11)	60
Belarus	200 (91-260)	18 (8-23)	69
Belgium	210 (96-270)	22 (10-29)	46
Belize	240 (110-320)	8.2 (3.6-11)	12
Benin	78 (34-100)	5.6 (2.4-7.4)	51
Bermuda	320 (140-420)	11 (4.7-14)	0
Bhutan	46 (20-61)	6.8 (3-9)	30
Bolivia	340 (150-440)	14 (6.4-19)	63
Bosnia and Herzegovina	90 (40-120)	10 (4.5-13)	28
Botswana	150 (65-200)	8.4 (3.7-11)	35
Brazil	220 (100-290)	13 (5.9-17)	71
Brunei	94 (42-120)	8.1 (3.6-11)	53
Bulgaria	100 (46-130)	11 (5-15)	41
Burkina Faso	140 (62-190)	9.1 (4-12)	37
Burundi	51 (22-67)	2.9 (1.3-3.8)	46
Cambodia	200 (89-260)	9.8 (4.3-13)	23
Cameroon	87 (38-110)	6.9 (3-9.1)	74
Canada	450 (210-580)	20 (9-25)	68
Cape Verde	68 (30-90)	5.6 (2.4-7.4)	13
Central African Republic	72 (31-95)	3.8 (1.6-4.9)	60

Chad	120 (54-160)	8.7 (3.8-11)	59
Chile	320 (150-410)	20 (9-25)	78
China	260 (120-330)	19 (9-25)	53
Colombia	300 (140-390)	13 (6.1-17)	82
Comoros	33 (14-44)	1.6 (0.7-2.2)	82
Congo	110 (48-140)	6.5 (2.9-8.5)	90
Costa Rica	190 (85-250)	8.5 (3.8-11)	66
Cote d'Ivoire	71 (31-93)	4.8 (2.1-6.3)	71
Croatia	110 (50-150)	12 (5.2-15)	36
Cuba	310 (140-400)	11 (4.7-14)	56
Cyprus	160 (71-210)	16 (7.1-21)	57
Czech Republic	140 (62-180)	16 (7.3-21)	30
Democratic Republic of the Congo	81 (36-110)	3.9 (1.7-5.1)	83
Denmark	140 (63-190)	13 (5.9-17)	38
Djibouti	180 (80-240)	11 (4.8-14)	0
Dominica	100 (46-140)	3.7 (1.6-4.9)	0
Dominican Republic	310 (140-400)	12 (5.5-16)	78
Ecuador	260 (120-340)	14 (6.4-18)	71
Egypt	260 (120-330)	15 (6.8-19)	91
El Salvador	220 (99-290)	10 (4.6-14)	60
Equatorial Guinea	82 (36-110)	4.2 (1.8-5.6)	66
Eritrea	150 (68-200)	9 (3.9-12)	49
Estonia	160 (73-210)	14 (6.3-18)	51
Ethiopia	74 (32-97)	5.1 (2.2-6.8)	49
Federated States of Micronesia	6.4 (2.8-8.4)	0.26 (0.11-0.35)	0
Finland	230 (100-300)	15 (6.9-20)	41
France	180 (82-230)	17 (7.7-21)	58
Gabon	70 (31-93)	3.5 (1.5-4.6)	72
Georgia	120 (53-150)	12 (5.6-16)	51
Germany	170 (78-220)	19 (8.6-24)	45
Ghana	64 (28-84)	5.6 (2.5-7.4)	67
Greece	140 (62-180)	14 (6.5-19)	68
Greenland	250 (110-330)	12 (5.2-15)	0
Grenada	55 (24-73)	1.8 (0.78-2.4)	0
Guam	0 (0-0)	0 (0-0)	0
Guatemala	170 (77-220)	10 (4.6-14)	55
Guinea	67 (29-89)	4.1 (1.8-5.5)	54
Guinea-Bissau	60 (26-80)	4.4 (1.9-5.8)	60
Guyana	190 (82-250)	6.8 (3-8.9)	23

Haiti	290 (130-380)	9.9 (4.4-13)	70
Honduras	180 (80-240)	9 (4-12)	50
Hungary	110 (50-150)	14 (6.1-18)	35
Iceland	150 (65-190)	12 (5.2-15)	71
India	72 (32-93)	14 (6.2-18)	69
Indonesia	180 (82-240)	8.3 (3.7-11)	83
Iran	330 (150-420)	22 (10-28)	73
Iraq	330 (150-420)	20 (8.9-25)	72
Ireland	150 (64-190)	9 (4-12)	48
Israel	210 (96-270)	20 (9.2-26)	73
Italy	110 (51-150)	15 (6.6-19)	46
Jamaica	200 (89-260)	7.4 (3.3-9.7)	62
Japan	280 (130-350)	23 (11-29)	83
Jordan	410 (190-530)	22 (9.9-28)	75
Kazakhstan	140 (65-180)	17 (7.8-22)	56
Kenya	64 (28-84)	4.1 (1.8-5.4)	40
Kiribati	0 (0-0)	0 (0-0)	0
Kuwait	550 (260-690)	30 (14-38)	92
Kyrgyzstan	160 (72-210)	15 (6.8-20)	51
Laos	160 (71-210)	8.1 (3.5-11)	19
Latvia	160 (73-210)	14 (6.3-18)	45
Lebanon	410 (190-510)	23 (11-29)	76
Lesotho	130 (55-170)	7.6 (3.3-10)	15
Liberia	21 (9.1-28)	1.6 (0.67-2.1)	77
Libya	210 (91-270)	13 (5.7-17)	53
Lithuania	150 (67-190)	15 (6.6-19)	48
Luxembourg	250 (110-320)	17 (7.8-22)	34
Macedonia	110 (49-140)	12 (5.4-16)	46
Madagascar	83 (36-110)	4.3 (1.9-5.6)	33
Malawi	78 (34-100)	4.5 (1.9-5.9)	20
Malaysia	230 (110-300)	11 (5.1-15)	77
Maldives	230 (110-300)	13 (5.7-16)	1.00E+02
Mali	110 (47-140)	9.4 (4.1-12)	36
Malta	130 (57-170)	11 (4.8-14)	85
Marshall Islands	0 (0-0)	0 (0-0)	0
Mauritania	180 (78-230)	10 (4.6-14)	35
Mauritius	36 (16-48)	1.8 (0.77-2.3)	79
Mexico	280 (130-360)	19 (8.6-24)	73
Moldova	110 (49-150)	11 (5-15)	26

Mongolia	180 (82-230)	18 (8.2-23)	54
Montenegro	84 (37-110)	8.9 (3.9-12)	37
Morocco	160 (70-210)	11 (5.1-15)	62
Mozambique	84 (36-110)	4.3 (1.9-5.7)	51
Myanmar	180 (78-230)	10 (4.5-13)	44
Namibia	170 (74-220)	9.3 (4.1-12)	23
Nepal	76 (33-99)	9.9 (4.4-13)	32
Netherlands	230 (100-290)	22 (9.9-28)	56
New Zealand	110 (48-150)	5.3 (2.3-7)	63
Nicaragua	120 (54-160)	7.2 (3.1-9.5)	46
Niger	150 (66-200)	11 (4.6-14)	41
Nigeria	130 (56-170)	8 (3.5-10)	58
North Korea	270 (120-350)	15 (6.7-20)	53
Northern Mariana Islands	0 (0-0)	0 (0-0)	0
Norway	140 (62-180)	13 (5.8-17)	40
Oman	270 (120-350)	16 (7.3-21)	34
Pakistan	140 (64-180)	16 (7.2-21)	65
Palestine	280 (130-360)	17 (7.6-22)	54
Panama	150 (67-200)	6.7 (2.9-8.8)	59
Papua New Guinea	93 (40-120)	3.5 (1.5-4.7)	39
Paraguay	260 (120-340)	10 (4.5-13)	67
Peru	380 (170-490)	15 (6.9-19)	70
Philippines	230 (100-290)	9.1 (4.1-12)	74
Poland	160 (73-210)	16 (7-20)	35
Portugal	170 (75-220)	13 (5.7-16)	55
Puerto Rico	220 (99-290)	8.1 (3.6-11)	61
Qatar	410 (200-520)	30 (14-37)	88
Romania	140 (60-180)	12 (5.4-16)	38
Russian Federation	180 (85-240)	18 (8.4-23)	61
Rwanda	63 (27-84)	2.9 (1.2-3.8)	34
Saint Lucia	76 (33-100)	2.8 (1.2-3.7)	0
Saint Vincent and the Grenadines	57 (24-75)	2 (0.87-2.7)	0
Samoa	0 (0-0)	0 (0-0)	0
Sao Tome and Principe	3.3 (1.4-4.4)	0.25 (0.11-0.33)	0
Saudi Arabia	320 (150-400)	24 (11-31)	78
Senegal	120 (51-150)	10 (4.4-13)	76
Serbia	140 (62-180)	12 (5.5-16)	46
Seychelles	0.00078 (0.00033-0.001)	4e-05 (1.7e-05-5.3e-05)	0
Sierra Leone	42 (18-55)	3 (1.3-3.9)	48

Singapore	300 (140-370)	26 (12-33)	1.00E+02
Slovakia	110 (47-140)	12 (5.4-16)	18
Slovenia	97 (43-130)	11 (4.7-14)	25
Solomon Islands	34 (15-45)	1.3 (0.56-1.7)	50
Somalia	140 (63-190)	8.2 (3.6-11)	40
South Africa	180 (81-240)	9.4 (4.2-12)	62
South Korea	330 (160-420)	31 (15-38)	88
South Sudan	95 (41-130)	5.5 (2.4-7.3)	50
Spain	170 (79-220)	16 (7.3-21)	63
Sri Lanka	110 (49-150)	5.6 (2.4-7.3)	49
Sudan	210 (92-270)	11 (4.8-14)	65
Suriname	160 (69-210)	5.2 (2.3-6.8)	64
Swaziland	130 (56-170)	6.2 (2.7-8.1)	21
Sweden	190 (84-240)	14 (6.3-18)	46
Switzerland	150 (69-200)	14 (6.3-18)	41
Syria	350 (160-440)	19 (8.9-25)	55
Taiwan	420 (190-540)	21 (9.6-27)	87
Tajikistan	140 (62-180)	14 (6.4-19)	54
Tanzania	90 (39-120)	4.2 (1.8-5.6)	25
Thailand	270 (120-350)	12 (5.2-15)	47
The Bahamas	270 (120-350)	9.3 (4.1-12)	0
The Gambia	100 (43-130)	7.1 (3.1-9.3)	54
Timor-Leste	120 (51-150)	5.4 (2.4-7)	42
Togo	85 (37-110)	5.9 (2.6-7.8)	67
Tonga	0 (0-0)	0 (0-0)	0
Trinidad and Tobago	210 (90-270)	7 (3.1-9.2)	67
Tunisia	170 (75-220)	11 (5-15)	55
Turkey	280 (130-350)	19 (8.6-24)	63
Turkmenistan	170 (75-210)	18 (8-23)	64
Uganda	44 (19-58)	2.5 (1.1-3.3)	47
Ukraine	150 (69-200)	13 (5.8-17)	52
United Arab Emirates	460 (220-580)	30 (14-38)	93
United Kingdom	280 (130-350)	19 (8.7-24)	74
United States	300 (140-390)	19 (8.5-24)	62
Uruguay	190 (84-250)	12 (5.3-16)	50
Uzbekistan	180 (79-230)	16 (7-20)	64
Vanuatu	13 (5.8-18)	0.52 (0.22-0.69)	0
Venezuela	240 (110-310)	14 (6.1-17)	77
Vietnam	210 (92-270)	13 (5.6-16)	66

Virgin Islands, U.S.	130 (56-170)	4.4 (1.9-5.8)	0
Yemen	240 (110-310)	15 (6.8-20)	47
Zambia	84 (37-110)	5.7 (2.5-7.5)	59
Zimbabwe	92 (40-120)	6 (2.6-7.9)	38

Table S7. Urban sums of NO_2-attributable paediatric asthma incidence per 100k children and percentage of NO_2-attributable incidence assuming counterfactual concentrations of 0ppb, 2ppb, and 5ppb for 125 major cities. The estimates shown are derived using the central mean relative risk (RR) value from Khreis et al. (2017), with the 95% uncertainty intervals reflecting uncertainty in the RR shown in parentheses for the number of cases. Results are rounded to 2 significant figures.

	0 ppb		2 ppb		5 ppb	
city	**Cases per 100k per year**	**Percentage**	**Cases per 100k per year**	**Percentage**	**Cases per 100k per year**	**Percentage**
Abidjan	250 (110-330)	17 (7.4-22)	180 (82-240)	12 (5.5-16)	95 (43-120)	6.4 (2.9-8.2)
Accra	170 (74-220)	15 (6.5-20)	120 (52-150)	10 (4.6-14)	51 (23-65)	4.5 (2-5.8)
Addis Ababa	280 (130-370)	22 (9.9-29)	230 (100-290)	18 (8-23)	140 (67-180)	11 (5.2-14)
Ahmedabad	170 (78-210)	33 (15-42)	150 (69-180)	29 (13-36)	110 (55-140)	22 (11-28)
Alexandria	470 (210-600)	27 (13-35)	390 (180-490)	23 (11-29)	280 (140-350)	17 (8.1-21)
Algiers	350 (150-450)	20 (8.8-26)	270 (120-350)	15 (6.9-20)	160 (73-200)	9 (4.2-11)
Amman	580 (270-750)	30 (14-39)	500 (230-630)	26 (12-33)	370 (180-470)	19 (9.3-24)
Ankara	480 (220-610)	32 (15-41)	410 (190-520)	28 (13-35)	320 (150-390)	21 (10-27)
Asyut	250 (110-330)	14 (6.2-19)	170 (75-220)	9.7 (4.3-13)	60 (27-76)	3.4 (1.5-4.3)
Baghdad	490 (220-630)	30 (13-38)	420 (190-530)	25 (12-32)	310 (150-390)	19 (8.8-23)
Bandung	520 (230-670)	23 (11-30)	420 (190-530)	19 (8.7-24)	280 (130-350)	13 (5.9-16)
Bangalore	160 (75-210)	31 (14-40)	140 (65-180)	27 (12-34)	110 (50-130)	20 (9.6-25)
Bangkok	580 (260-740)	26 (12-33)	470 (220-600)	21 (9.6-27)	330 (160-410)	15 (6.9-18)
Barcelona	280 (130-360)	26 (12-33)	230 (110-300)	21 (9.7-27)	160 (76-200)	15 (6.9-19)
Beijing	620 (310-760)	47 (23-57)	560 (280-680)	42 (21-51)	470 (240-570)	36 (18-43)
Belo Horizonte	440 (200-570)	26 (12-34)	370 (170-470)	22 (10-28)	260 (120-330)	15 (7.3-19)
Bogota	680 (310-870)	31 (14-39)	580 (270-730)	26 (12-33)	440 (210-540)	20 (9.4-24)
Buenos Aires	480 (220-620)	31 (14-39)	410 (190-520)	26 (12-33)	310 (150-390)	20 (9.4-24)
Cairo	450 (210-580)	26 (12-33)	370 (180-470)	21 (10-27)	260 (130-320)	15 (7.3-18)
Caracas	450 (210-590)	26 (12-33)	370 (170-480)	21 (9.7-27)	260 (120-330)	15 (6.9-18)
Casablanca	350 (160-450)	25 (11-32)	290 (130-370)	21 (9.5-26)	200 (94-250)	14 (6.7-18)
Chengdu	430 (200-550)	34 (16-43)	380 (180-470)	30 (14-37)	290 (140-360)	23 (11-29)
Chennai	130 (60-170)	26 (12-33)	110 (50-140)	21 (9.7-27)	76 (36-96)	15 (7-19)
Chicago	550 (250-690)	34 (16-43)	470 (220-600)	29 (14-37)	370 (180-460)	23 (11-28)
Chittagong	140 (63-180)	21 (9.6-28)	110 (51-140)	17 (7.7-22)	71 (33-89)	11 (5-13)
Chongqing	470 (220-590)	37 (17-46)	410 (200-510)	32 (15-40)	330 (160-400)	26 (13-32)
Cologne	290 (140-370)	32 (15-41)	250 (120-320)	28 (13-35)	190 (93-240)	21 (10-27)
Colombo	280 (120-370)	14 (6.2-19)	190 (86-250)	9.8 (4.3-13)	86 (39-110)	4.3 (2-5.5)
Dallas	510 (230-650)	30 (14-39)	430 (200-550)	26 (12-33)	320 (150-400)	19 (9.2-24)
Dar es Salaam	220 (92-290)	11 (4.5-14)	120 (54-160)	6 (2.6-7.9)	29 (13-38)	1.4 (0.65-1.9)
DC	460 (210-600)	27 (12-35)	390 (180-490)	23 (10-29)	280 (130-350)	16 (7.7-20)
Dhaka	180 (82-230)	27 (12-34)	150 (70-190)	22 (10-28)	110 (51-130)	16 (7.5-19)

Dubai	580 (270-730)	38 (18-48)	510 (250-640)	33 (16-42)	410 (200-510)	27 (13-33)
Faisalabad	240 (110-310)	28 (13-36)	200 (92-250)	23 (11-30)	140 (68-180)	17 (7.9-21)
Fuzhou	410 (190-520)	31 (14-39)	350 (160-440)	26 (12-33)	270 (130-330)	20 (9.6-25)
Guadalajara	450 (210-580)	30 (14-38)	380 (180-490)	25 (12-32)	290 (140-360)	19 (9-24)
Guangzhou	480 (230-600)	38 (18-48)	420 (200-530)	33 (16-41)	340 (170-420)	27 (13-33)
Hangzhou	500 (240-630)	38 (18-48)	440 (210-550)	34 (16-42)	360 (180-440)	28 (14-34)
Hanoi	420 (190-540)	25 (11-32)	350 (160-440)	21 (9.5-26)	240 (110-300)	14 (6.7-18)
Harbin	510 (250-640)	41 (20-51)	460 (220-560)	37 (18-45)	380 (190-460)	30 (15-37)
HCMC	480 (220-610)	29 (13-37)	400 (190-510)	24 (11-31)	300 (140-370)	18 (8.7-22)
Hefei	470 (220-590)	37 (17-46)	410 (200-510)	32 (15-40)	330 (160-410)	26 (13-31)
Hong Kong	500 (240-620)	39 (18-48)	440 (210-540)	34 (17-42)	360 (180-430)	28 (14-34)
Houston	480 (220-610)	29 (13-37)	400 (190-510)	24 (11-31)	300 (140-370)	18 (8.3-22)
Hyderabad	150 (66-190)	28 (13-36)	120 (57-160)	24 (11-30)	90 (43-110)	17 (8.3-22)
Istanbul	540 (260-680)	36 (17-46)	470 (230-590)	32 (15-39)	380 (190-460)	25 (12-31)
Jaipur	130 (59-170)	26 (12-33)	110 (49-140)	21 (9.7-27)	75 (35-95)	15 (6.9-19)
Jakarta	470 (210-620)	21 (9.5-28)	370 (170-480)	17 (7.7-22)	230 (110-290)	10 (4.9-13)
Jeddah	410 (190-530)	32 (15-41)	360 (170-450)	27 (13-35)	270 (130-340)	21 (10-26)
Johannesburg	420 (190-550)	21 (9.4-28)	330 (150-430)	17 (7.5-22)	210 (95-260)	10 (4.7-13)
Kabul	460 (210-590)	28 (13-36)	380 (180-490)	23 (11-30)	280 (130-350)	17 (7.9-21)
Kano	350 (160-460)	22 (9.8-29)	280 (130-360)	17 (7.9-22)	180 (82-220)	11 (5.1-14)
Kanpur	110 (51-150)	23 (10-31)	92 (42-120)	19 (8.6-24)	61 (28-78)	13 (5.8-16)
Karachi	300 (140-380)	36 (17-45)	260 (120-320)	31 (15-39)	210 (100-250)	25 (12-31)
Kathmandu	170 (76-220)	24 (11-31)	140 (62-180)	19 (8.6-24)	91 (42-110)	13 (5.9-16)
Khartoum	410 (180-530)	21 (9.5-28)	320 (150-420)	17 (7.6-22)	200 (92-260)	10 (4.8-13)
Kinshasa	450 (200-580)	22 (9.6-28)	350 (160-460)	17 (7.8-22)	230 (110-290)	11 (5.1-14)
Kolkata	120 (57-160)	25 (11-32)	100 (47-130)	20 (9.5-26)	70 (33-87)	14 (6.7-18)
Kuala Lumpur	620 (280-790)	29 (13-37)	520 (240-660)	25 (11-31)	380 (180-480)	18 (8.6-23)
Lagos	320 (140-420)	20 (9-26)	250 (110-320)	16 (7.2-20)	150 (71-190)	9.8 (4.5-12)
Lahore	240 (110-300)	27 (12-35)	200 (91-250)	23 (11-29)	140 (67-180)	17 (7.8-21)
Lima	810 (370-1000)	33 (15-41)	690 (330-870)	28 (13-35)	540 (260-660)	22 (10-27)
London	510 (240-650)	34 (16-43)	440 (210-560)	29 (14-36)	350 (170-430)	23 (11-28)
Los Angeles	600 (290-760)	38 (18-47)	530 (260-660)	33 (16-41)	430 (210-530)	27 (13-33)
Luanda	430 (190-560)	21 (9.2-27)	340 (150-430)	16 (7.3-21)	200 (94-260)	9.8 (4.5-12)
Lucknow	120 (55-160)	25 (11-32)	99 (45-130)	20 (9.1-26)	68 (32-86)	14 (6.4-17)
Madrid	350 (160-440)	31 (14-40)	300 (140-370)	27 (13-34)	230 (110-280)	21 (9.8-26)
Manchester	410 (180-520)	28 (13-36)	340 (160-430)	23 (11-30)	250 (120-310)	17 (8-21)
Manila	650 (300-830)	26 (12-33)	530 (250-680)	21 (9.9-27)	380 (180-470)	15 (7.2-19)
Medan	360 (160-470)	16 (7.1-21)	260 (120-340)	12 (5.2-15)	120 (56-160)	5.6 (2.6-7.2)
Mexico City	590 (280-740)	39 (19-49)	520 (250-650)	35 (17-43)	430 (210-520)	28 (14-35)

Miami	390 (170-510)	24 (11-31)	320 (140-410)	20 (8.9-25)	210 (99-270)	13 (6.2-17)
Milan	260 (120-330)	33 (15-41)	220 (110-280)	28 (13-35)	170 (83-220)	22 (10-27)
Monterrey	480 (220-610)	31 (14-40)	410 (190-520)	27 (13-34)	310 (150-390)	20 (9.8-25)
Moscow	450 (220-560)	45 (22-56)	410 (200-500)	40 (20-50)	340 (170-410)	34 (17-41)
Mumbai	150 (69-190)	29 (14-38)	130 (59-160)	25 (12-32)	94 (45-120)	19 (8.9-23)
Nagoya	390 (180-490)	31 (14-40)	330 (150-420)	27 (12-34)	250 (120-310)	20 (9.7-25)
Nairobi	300 (130-390)	19 (8.1-24)	230 (100-290)	14 (6.3-18)	130 (57-160)	7.8 (3.5-9.9)
Nanjing	500 (240-620)	39 (19-49)	440 (210-540)	35 (17-43)	360 (180-440)	28 (14-35)
Naples	150 (66-190)	20 (8.6-26)	110 (51-150)	15 (6.7-19)	67 (31-85)	8.7 (4-11)
New Delhi	170 (78-210)	33 (15-42)	140 (68-180)	28 (13-36)	110 (54-140)	22 (11-27)
NYC	600 (290-760)	37 (17-46)	530 (260-660)	32 (16-40)	420 (210-520)	26 (13-32)
Orlu	150 (64-200)	10 (4.3-14)	83 (36-110)	5.6 (2.4-7.4)	8.8 (3.9-11)	0.59 (0.27-0.77)
Osaka	400 (190-510)	33 (15-42)	340 (160-430)	28 (13-36)	270 (130-330)	22 (11-27)
Paris	410 (200-520)	38 (18-47)	360 (180-450)	33 (16-41)	290 (150-360)	27 (13-33)
Peshawar	170 (73-220)	19 (8.3-25)	130 (56-160)	14 (6.4-19)	70 (32-90)	7.9 (3.6-10)
Philadelphia	500 (230-630)	31 (14-39)	420 (200-540)	26 (12-33)	320 (150-400)	20 (9.4-25)
Pune	140 (65-180)	27 (12-35)	120 (55-150)	23 (11-29)	86 (40-110)	16 (7.7-21)
Qingdao	500 (230-630)	37 (17-46)	440 (210-540)	32 (15-40)	350 (170-430)	26 (13-32)
Quanzhou	330 (150-420)	25 (11-33)	270 (120-340)	21 (9.5-27)	190 (87-230)	14 (6.7-18)
Rangoon	350 (150-460)	21 (9.2-27)	270 (120-350)	16 (7.3-21)	170 (76-210)	9.8 (4.5-12)
Rawalpindi	230 (100-290)	26 (12-34)	190 (85-240)	22 (9.9-28)	130 (62-170)	15 (7.2-19)
Rio de Janeiro	430 (200-560)	26 (12-33)	360 (160-460)	21 (9.7-27)	250 (120-310)	15 (7-19)
Riyadh	470 (220-590)	36 (17-46)	410 (200-510)	32 (15-40)	330 (160-400)	25 (12-31)
San Diego	490 (220-620)	30 (14-38)	410 (190-520)	25 (12-32)	310 (150-390)	19 (8.9-24)
San Francisco	540 (250-690)	32 (15-41)	460 (220-590)	28 (13-35)	360 (170-440)	21 (10-26)
Santiago	580 (270-740)	35 (16-44)	510 (240-630)	30 (14-38)	400 (190-490)	24 (12-30)
Santo Domingo	560 (250-730)	23 (10-29)	450 (200-580)	18 (8.2-23)	290 (140-370)	12 (5.5-15)
Sao Paulo	550 (250-700)	32 (15-41)	470 (220-590)	27 (13-35)	360 (170-450)	21 (10-26)
Semarang	270 (120-360)	13 (5.5-17)	180 (78-230)	8.2 (3.6-11)	55 (25-71)	2.6 (1.2-3.3)
Seoul	490 (240-610)	45 (22-55)	440 (220-540)	40 (20-49)	370 (190-450)	34 (17-41)
Shanghai	710 (360-850)	52 (27-63)	650 (340-770)	48 (25-57)	560 (300-660)	41 (22-48)
Shantou	270 (120-350)	22 (9.6-28)	210 (95-270)	17 (7.7-22)	130 (60-170)	11 (4.9-14)
Shenyang	590 (290-730)	46 (22-56)	540 (270-650)	41 (21-50)	450 (230-540)	35 (18-42)
Singapore	330 (150-420)	29 (13-37)	280 (130-350)	24 (11-31)	200 (97-260)	18 (8.4-22)
Sohag	230 (99-310)	13 (5.7-18)	150 (66-200)	8.7 (3.8-11)	41 (19-53)	2.4 (1.1-3)
St Petersburg	390 (180-490)	39 (18-49)	340 (160-430)	34 (17-43)	280 (140-340)	28 (14-34)
Surabaya	390 (170-510)	18 (7.9-23)	290 (130-380)	13 (6-17)	150 (71-200)	7 (3.2-8.9)
Surakarta	300 (130-400)	14 (6.1-18)	210 (91-270)	9.5 (4.2-12)	72 (33-92)	3.3 (1.5-4.2)
Surat	130 (61-170)	26 (12-34)	110 (51-140)	22 (9.9-28)	78 (37-99)	15 (7.1-19)

Sydney	370 (160-490)	18 (7.8-23)	280 (120-360)	13 (6-17)	150 (68-190)	7.2 (3.3-9.1)
Taipei	600 (270-760)	30 (14-38)	510 (240-640)	25 (12-32)	380 (180-470)	19 (8.9-23)
Taiyuan	540 (260-670)	43 (21-54)	490 (240-600)	39 (19-48)	410 (200-490)	32 (16-39)
Tashkent	310 (140-410)	28 (13-36)	260 (120-340)	23 (11-29)	190 (89-240)	17 (7.8-21)
Tehran	590 (280-740)	40 (19-50)	520 (250-650)	35 (17-44)	430 (210-520)	29 (14-35)
Tianjin	610 (300-740)	47 (23-58)	550 (280-660)	43 (22-52)	470 (240-560)	36 (19-44)
Tokyo	470 (230-590)	38 (18-48)	420 (200-520)	34 (16-42)	340 (170-410)	27 (14-33)
Toronto	650 (300-840)	28 (13-36)	550 (250-700)	24 (11-30)	400 (190-500)	17 (8.2-22)
Varanasi	110 (49-140)	22 (9.8-29)	88 (40-110)	18 (7.9-23)	56 (26-71)	11 (5.2-14)
Wenzhou	340 (160-440)	26 (12-33)	280 (130-360)	21 (9.8-27)	200 (94-250)	15 (7-19)
Wuhan	490 (230-610)	40 (19-50)	430 (210-530)	35 (17-43)	350 (180-430)	29 (14-35)
Wuxi	510 (240-640)	40 (19-50)	450 (220-560)	35 (17-44)	370 (180-450)	29 (14-35)
Xiamen	480 (230-610)	35 (17-45)	420 (200-520)	31 (15-39)	330 (160-410)	25 (12-30)
Xi'an	550 (270-690)	44 (21-54)	500 (250-610)	39 (19-48)	420 (210-500)	33 (17-39)
Zhengzhou	560 (270-700)	42 (20-52)	500 (240-620)	38 (18-46)	410 (210-500)	31 (16-38)